



NASA Contractor Report 4137

Structureborne Noise Measurements on a Small Twin-Engine Aircraft

J. E. Cole III and K. F. Martini

**CONTRACT NAS1-18020
JUNE 1988**

{NASA-CR-4137) STRUCTUREBORNE NOISE
MEASUREMENTS ON A SMALL TWIN-ENGINE AIRCRAFT
{Cambridge Acoustical Associates) 71 p

CSCL 20A

H1/71

N88-23545

Unclas
0140052

NASA

NASA Contractor Report 4137

Structureborne Noise Measurements on a Small Twin-Engine Aircraft

J. E. Cole III and K. F. Martini
Cambridge Acoustical Associates, Inc.
Cambridge, Massachusetts

Prepared for
Langley Research Center
under Contract NAS1-18020



National Aeronautics
and Space Administration

Scientific and Technical
Information Division

1988

TABLE OF CONTENTS

	<u>Page</u>
I. INTRODUCTION	1
II. TEST CONFIGURATION	2
III. RESULTS	4
A. Data Presentation	4
B. Data Integrity	4
C. Comparison of Transfer Functions Measured by Reciprocal and Direct Methods	8
D. Results: Standard Configuration	10
E. Results: Parameter Sensitivity	11
1. Wing Attachment Bolt Torque	11
2. Mass of Simulated Wing Fuel	13
3. Interior Acoustic Volume Absorption	13
IV. CONCLUSIONS	15
FIGURES	17-33
REFERENCES	34
APPENDIX A: MODAL TEST EVALUATION OF LOW FREQUENCY WING DYNAMICS .	A-1
A.I INTRODUCTION	A-1
A.II PROCEDURE	A-1
A.III RESULTS	A-2
A. Freely-Supported Wing	A-2
B. Wing Attached to Fuselage	A-3
C. Parameter Sensitivity	A-3
1. Force Amplitude	A-3
2. Left-Hand and Right-Hand Wing Response .	A-4
3. Support Configuration	A-4
TABLES	A-6-7
FIGURES	A-8-13
APPENDIX B: MODE SHAPES FOR WING WITHOUT ENGINE MOUNT WHEN FREELY SUPPORTED	B-1-4
APPENDIX C: MODE SHAPES FOR WING WITH ENGINE MOUNT WHEN FREELY SUPPORTED	C-1-5

Table of Contents (Continued)

	<u>Page</u>
APPENDIX D: MODE SHAPES FOR WING WITH ENGINE MOUNT WHEN BOLTED TO FUSELAGE	D-1-4

I. INTRODUCTION

As part of our program to develop the analytical and experimental tools required to evaluate structureborne noise on propeller driven aircraft, tests were performed on a twin-engine Beechcraft Baron 58P aircraft housed at NASA Langley Research Center. Two major tests were performed on this aircraft, one in April 1986 and the other in November 1986. In addition shorter tests to verify instrumentation and test procedures were performed in December 1986, April 1987 and June 1987. All tests were performed at NASA Langley Research Center; technicians and other technical assistance were provided by NASA for these tests.

The overall objectives of the test program included the following: to obtain measurements to support and guide the development of analytical models of the structureborne noise path; and to evaluate the effects of structural parameters and path modifications on the noise in the aircraft cabin.

The April 1986 tests were designed to help define the structure through input mobility and loss factor measurements and to evaluate structural acoustic transfer functions (i.e., cabin sound pressure per structural excitation force) for the fuselage.

Tests performed in November 1986 were primarily designed to evaluate the effects of changes in the structural path on the noise field in the cabin. Results of these latter tests along with comparison with the previous measurements are discussed in this report.

II. TEST CONFIGURATION

Tests on the Beechcraft Baron were performed at NASA Langley Research Center in a semi-anechoic laboratory space. Acoustic absorption in the space was provided by approximately a dozen 32 square foot panels of 4 inch thick fiberglass batting positioned around the aircraft. In all tests the aircraft fuselage and wing were supported by large truck inner tubes that provided vibration isolation from the laboratory floor. The interior of the aircraft was fully trimmed with seats in place.

The fuselage of the Beechcraft Baron 58P was a new production unit that was complete except for instrumentation. The wings of the Baron obtained from a damaged aircraft were incomplete, having neither flaps nor internal fuel lines or fuel tank bladders. Damage in the form of wrinkling and loose rivets was found on several portions of the skin on each wing. A correct engine mount for the wing was not obtained; however, a similar mount was modified to fit the bolt locations on the wing. Engines were not present on the test aircraft.

The aircraft was structurally excited by means of a 4 ounce hammer instrumented with a PCB force gauge. Accelerations were measured using Bruel and Kjaer 4332 accelerometers and 2635 charge amplifiers, and calibration was performed using a GenRad type 1557 accelerometer calibrator. The interior and exterior acoustic fields of the aircraft were measured using Bruel and Kjaer 1/2 inch microphones and type 2209 sound level meters. Calibration of the microphones was performed by means of a GenRad type 1562 microphone calibrator.

The locations of the accelerometers and microphones are indicated on Fig. 1. The sound levels inside and outside the cabin were monitored using single microphones (transducers 1 and 6, respectively). Location 1 is over the right rear seat approximately 9 inches down from the ceiling and 11 inches in from the right rear window. Location 6 is approximately 12 inches above the top of the fuselage near the axial position of the internal microphone (i.e., location 1). The structural response was measured at several locations. Location 52, the outboard forward engine mount, was used to measure the drive point response. The fore-and-aft (i.e., thrust direction) response of the

carry-through structure of the main wing spar in the fuselage was measured at location 106. The third accelerometer (41) was attached externally to the fuselage and oriented outwardly. It was attached on the fuselage skin approximately 2 inches away from vertical and axial stiffeners. The accelerometer locations 52 and 41 as well as the microphone location 1 were also used in the set of tests performed during April 1986.

Signals from the transducers used in the tests were acquired and processed by a GenRad 2515 Computer aided test system. Data acquisition was triggered by the signal from the force gauge on the hammer. A bandwidth of 1000 Hz was used with a 2 Hz resolution for the calculated frequency response functions. Auto- and cross- spectra of the responses (i.e., acceleration and acoustic pressure) relative to the force excitation were calculated, printed, and saved on disk. Transfer of the saved data from the GenRad system to a VAX 11/780 system and then to a MicroVax system at NASA Langley permitted the calculated response data to be written on a DEC TK50 tape cassette. In this form the data could be loaded and further analyzed on the CAA MicroVax II computer.

III. RESULTS

A. Data Presentation

The frequency response data processed with two Hertz resolution display substantial variations with frequency due to system resonances and antiresonances. As a means of simplifying the presentation of these results, the data are averaged over one-third octave bands. A comparison of the narrow-band and one-third octave band data for the interior microphone and for the fuselage accelerometer is given in Fig. 2a.

While the broader bandwidth is useful for displaying global trends in the data more clearly, it hides the extent of the narrow band fluctuations of the data. One measure of these fluctuations is the standard deviation of the decibel levels within each one-third octave band. Results for the data of Fig. 2a are shown in Fig. 2b. The relatively high standard deviation at low frequencies is due to isolated resonances. In the frequency range between 100 and 500 Hz, the standard deviations of both transfer functions are approximately 5.6 dB which is the value obtained when the frequency dependence of the response has a Gaussian distribution.

B. Data Integrity

The integrity of the data taken during the November tests has been evaluated in several ways. The signal-to-noise ratio (S/N) of the data is examined by subtracting the auto-spectrum of the noise from that of the signal for the various sensors, test configurations, and excitation locations. Of particular interest are the accelerometers away from the drive point and the microphones. Although the results vary somewhat, several general statements regarding the S/N in one-third octave bands can be made.

1. When the wing is connected to the fuselage but not mass loaded, the S/N of the fuselage accelerometers and microphones exceeds 10 dB throughout the frequency range above 40 Hz and generally exceeds 20 dB above 63 Hz.
2. Mass loading the wing tends to reduce the S/N somewhat, the greatest changes being found in the microphone signals when the wing is excited along the spar. For example when point 53 (forward spar inboard of the engine)

is excited the S/N of the microphone exceeds 10 dB above 63 Hz and 20 dB above 160 Hz.

3. When the wing is disconnected from the fuselage, the interior cabin microphone S/N exceeds 10 dB above 62 Hz. Ratios of S/N exceeding 20 dB are achieved above 125 Hz without mass loading; however, the level of S/N is never as high as 20 dB when the wing is mass loaded. The data presented in the figures in this report have a minimum S/N of 10 dB. Rather than setting a uniform low frequency limit for all results to have at least 10 dB S/N, the data shown on the individual figures have been plotted over the maximum frequency range permitted for each set of data.

Because the testing is performed using broadband excitation, an additional requirement is imposed on the data, namely high coherence between input and output signals. This is particularly important when reciprocity between input and output is invoked. Reciprocity generally requires linearity in the test system, and in its simplest form means that response and excitation locations may be interchanged without altering the transfer function, that is,

$$H_{xy}' = y'/x = H_{yx}' = y/x'$$

where y is the output, x is the input, and the apostrophe denotes the transfer location. This equality is only true when the output and input are perfectly coherent, since by definition the ordinary coherence function is given by

$$\gamma^2 = \frac{G_{xy} G_{yx}^*}{G_{xx} G_{yy}}$$

where G_{xy} is the cross-spectrum of the input and output signals and G_{xx} and G_{yy} are the respective auto-spectra. When defined in terms of the cross-spectrum, the direct and reciprocal transfer functions are

$$H_{xy} \equiv \frac{G_{xy}}{G_{xx}}$$

$$H_{yx} \equiv \frac{G_{yx}}{G_{yy}}$$

By substituting these results into the definition of the coherence function, we see that reciprocity requires that the coherence function be unity, that is,

$$H_{xy} = \gamma^2 (H_{yx}^*)^{-1}$$

In the broadband testing performed attempts were made to obtain high coherence between all signal pairs throughout the frequency range of interest. As a practical matter however none of the tests resulted in transfer functions having unity coherence throughout the frequency range from 0 to 1000 Hertz. In some tests regions of low coherence were unavoidable (e.g., reciprocal tests using the acoustic source below 100 Hz), and in general the coherence is low near system antiresonances. In broad terms however the coherence of most of the test data is 0.90 or greater.

Results of two independent tests performed within one hour of each other for the same test configuration showing the one-third octave-band transfer function between the interior microphone and the engine mount drive-point accelerometer are given on Fig. 3. Although the frequency dependence of both curves is similar, level differences reaching 3 dB at some frequencies are found.

Variability in the magnitude displayed on Fig. 3 is not considered to be important for the present purposes; however, other tests repeated at various times during the test program give results with somewhat greater differences. On occasion sequential tests on the aircraft resulted in transfer functions having similar frequency dependences but being shifted in amplitude by as much as 3-5 dB. Some of these differences are likely due to variations in coherence among the tests.

In one repeated test the aircraft configuration was not changed; however, a different tip was used on the instrumented hammer. Several interchangeable tips are available to the hammer including soft rubber and hard teflon. Although the total force imparted to the structure is nominally the same for each tip, the frequency spectrum of the applied force varies. Tests of the variability due to different tips were made using a freely suspended mass

with attached accelerometer. The transfer function of applied force to acceleration should be equal to the mass used in the test. This test was performed with both one and ten pound weights using the GenRad 2515 system to acquire and process the data. The variability among results obtained from single hammer impacts was as high as 30 percent (i.e., 2.2 dB), while the variability was under 20 percent (i.e., 1.6 dB) when averaged over 5 impacts.

During these mass law tests, there were some impacts that caused an overload warning in the GenRad 2515 analyzer. In some of these cases the transfer function obtained from single impacts appeared to be valid (i.e., within the variance of tests without the overload warning). The transfer function derived from other such impacts however was substantially different (e.g., 6 dB). During the normal testing procedure involving several data channels, the transfer functions from multiple (e.g., 10) impacts are averaged. Transfer functions averaged over this number of impacts was found to be well defined and not subject to significant change with more than 10 impacts. In this mode of operation a warning message appears when a specific impact triggers the overload condition; however, the message disappears as soon as a subsequent impact does not overload the system. Although the intent during testing was to minimize conditions leading to the overload warning, it is possible that some of the variance in results obtained from repeated tests is due to specific impacts triggering an overload condition.

An independent test of the acoustic data is obtained by comparison with a simple analytical model. Shown on Fig. 4 is the difference between exterior and interior of sound pressure levels of the fuselage, the excitation being provided by a hammer impacting the detached wing. In this figure the exterior pressure is measured by the microphone on top of the fuselage near the location of the interior microphone. The line drawn through the spectrum is the low frequency transmission loss (i.e., the mass law) for random incidence through an infinite plate (Ref. 1),

$$TL = -17 + 15 \log_{10}(\rho_s hf)$$

where ρ_s is the plate density in kg/m^3 and h is the plate thickness in m. The slope of the measurements is consistent with this model. Furthermore, the plate thickness inferred from the data of 0.033 inches is reasonable for the fuselage given the presence of stringers and frames on the 0.020 inch thick skin.

C. Comparison of Transfer Functions Measured by Reciprocal and Direct Methods

Initial measurements of transfer functions between cabin pressure and force applied to the fuselage and wing were made using a reciprocal technique. The volume acceleration of a speaker (\ddot{Q}) located in the cabin was determined using electro-acoustic reciprocity. With this excitation the structural acceleration (\ddot{w}) at points on the fuselage and wing was determined. Assuming system linearity and perfect signal coherence, structural-acoustic reciprocity then allows the ratio of structural acceleration to volume acceleration between the two points to be equated to the cabin acoustic pressure per structural force excitation (see Ref. 2) that is,

$$\ddot{w}'/\ddot{Q} = p'/F$$

Direct measurement of the transfer function (i.e., measurement of p' and F) was made at several points during the initial set of tests. Narrow-band transfer functions between cabin locations and points on the fuselage were measured using both direct and reciprocal approaches. Subsequent testing made use of the direct method exclusively.

In both testing methods sufficient excitation amplitudes were maintained to provide adequate signal-to-noise ratios at the response sensors (i.e., greater than 20 dB over most of the frequency range of interest). The reciprocal method has the advantages of permitting steady excitation and of allowing multi-directional transfer functions to be easily measured through orientation of the small accelerometers. Its primary disadvantage however is the need to measure three separate transfer functions to determine

one structural acoustic transfer function (i.e., two transfer functions to calibrate the acoustic source in situ and one transfer function involving the structural acceleration). In view of the need for high coherence between each of the signals in each of the three transfer functions, this disadvantage reduces in practice the reliability of transfer functions derived by reciprocal testing. The direct test using the transient hammer excitation was found to be a simple method for obtaining the transfer function in a single measurement. As discussed above however non-uniform hammer impacts may have influenced the ability to achieve repeatability due to peculiarities in the signal acquisition system.

The one-third octave band transfer functions between the cabin pressure (location 1) and an excitation force at the forward wing attachment bolt (location 12) measured using both reciprocal and direct methods are compared on Fig. 5a. These functions were measured during the same test sequence. Above approximately 30 Hz reasonable agreement is obtained between these two results, although based on low coherence below 100 Hz due to both acoustic and hammer source strengths, agreement in this range is somewhat fortuitous.

Another comparison of transfer functions measured by both methods during the same test sequence is shown on Fig. 5b. In this case the location of the cabin pressure is the same; however, the structural location (Point 22) is on the stiffened wing skin near the fuselage. The direct transfer function is the RMS average of two-independent tests made sequentially using different hammer tips. A mean difference between the two direct test results is approximately 4 dB and may reflect in part differences in signal coherence. Focusing on the region above 100 Hz where both signal coherence and signal-to-noise ratios were high, there is somewhat less agreement between both test results than shown on the previous figure for excitation of the fuselage. No convincing explanation has been found for the somewhat poorer agreement obtained between direct and reciprocal results using structural locations on the wing.

One possible reason for disagreement between reciprocal and direct measurements on the Baron is nonlinear behavior of the structure. Several measurements of transfer mobilities on the wing at differing force amplitudes were made to examine this issue (see Appendix A). Force amplitudes were varied by a factor of approximately ten. Little change in the transfer accelerance along the wing was found except for regions near antiresonances where the signal-to-noise ratio was enhanced at the higher impact level. Non-linear behavior is therefore not indicated as the reason for the differences between direct and reciprocal measurements shown on Figs. 5a and 5b.

Because of the low coherence associated with the acoustic source characteristics below 100 Hz and the existence of regions of both low signal-to-noise and coherence in the other two transfer functions required to make the measurement, less confidence is placed in the results of the reciprocal testing. Furthermore, in the direct testing performed subsequent to the reciprocal tests, more parameters were controlled (e.g., bolt torque). Results of the tests performed in November 1986 are therefore used for comparison with analysis and for drawing conclusions regarding structureborne transmission on this aircraft.

D. Results: Standard Configuration

In its standard test configuration the Beechcraft Baron with one attached wing is vibration isolated from the floor of the building on truck inner tubes. The four wing bolts are tightened with a torque of 50 ft-lb (the standard configuration), and measurements are made of the acceleration and interior sound pressure at the locations indicated on Fig. 1. Excitation of the aircraft by means of the instrumented hammer occurred throughout the tests at several locations also indicated on Fig. 1.

The resulting cabin pressures per force applied to various locations on the wing and fuselage are shown on Fig. 6a and 6b. With the exception of the frequency range near 50 Hz little difference is found in the pressure when the force is applied to the engine mount (point 52) or to the skin

outboard of the engine mount (point 26). It should be noted that test results using point 26 have peculiarities that appear to be associated with the damaged (i.e., wrinkled) nature of the skin in this area of the wing. Substantially lower pressures are obtained throughout the frequency range (and especially below 125 Hz) when the force is applied at the fuselage forward bolt location (point 12) than when applied to the engine mount. In part this difference is due to fundamental vibrational modes of the wing structure (see Appendix A) that are excited when the engine mount is driven. The effect of these resonances on the cabin pressure is particularly evident in the low frequency peak at approximately 40 Hz. The results shown on Fig. 6b for excitations of the forward wing spar inboard and outboard of the engine mount (points 53 and 54) are nearly identical. The somewhat higher levels at point 22 compared with those of the April 1986 tests (shown on Fig. 5b) most likely reflect the more closely controlled bolt torque during the November tests.

The acceleration response at three locations is shown on Fig. 7a for an excitation at the engine mount. Compared with the drive-point response, the acceleration at the fuselage sidewall is down 30-40 dB above 100 Hz while that of the highly stiffened main spar carry-through structure is down an additional 10-20 dB in the same frequency range. The drive-point acceleration of the engine mount is high at frequencies below 500 Hz compared with the drive-point acceleration of the fuselage at the bolt attachment point (see Fig. 7b). At this point the fuselage structure behaves on average as a stiffness throughout the frequency range above 80 Hz.

E. Results: Parameter Sensitivity

1. Wing Attachment Bolt Torque

When the wing is force excited, contributions to the interior cabin pressure arrive via the structureborne path (i.e., the subject of the test) as well as via the flanking exterior path through the air and fuselage sidewall. As a means of determining the relative magnitude of these two paths, a baseline test with the wing detached from the fuselage was performed. Both wing and fuselage were independently soft-mounted on

inner tubes with approximately a foot of lateral distance separating the wing and fuselage mating surfaces. The same excitation of the wing as used in all other tests was provided, namely, a hammer impulse to the engine mount at point 52. The difference between the interior and exterior pressures measured with the wing attached and with the wing detached are given on Fig. 8. The presence of the fundamental wing resonances has a substantial effect on the interior pressure at frequencies below 50 Hz (see Fig. 6) in the attached configuration. In the frequency range above 80 Hz the difference in interior pressure is approximately 15 dB on average.

This level is taken to represent the difference between structureborne and airborne flanking paths to the cabin interior in the tests. Based on this result, the maximum alteration in the structureborne path that can be measured from the tests is somewhat less than 15 dB. Stated differently, since the detached wing is perfectly isolated structurally from the fuselage, the effectiveness of attachment compliance could only be examined until the interior level was reduced to that of the airborne flanking path (i.e., a 15 dB reduction at most). Further reduction in the flanking path would require isolation of the vibrating surface of the wing from the air. An elegant but impractical means to accomplish this would be to test the pressurized fuselage in a vacuum chamber.

The effect of the torque on the attachment bolts is shown on Fig. 9. The baseline for this comparison is the cabin pressure measured with the four bolts in place and tightened to a torque of 50 ft-lb. The two other conditions are (1) the addition of the shear tab bolt at 50 ft-lb and (2) the increase in torque of all five bolts to 150 ft-lb. The presence of the shear tab bolt is seen in the results below 50 Hz; however, at higher frequencies any effect of this bolt or of the torque within this range is negligible (i.e., within the repeatability uncertainty of the tests).

2. Mass of Simulated Wing Fuel

Fuel tanks along the leading edge and interior of each of the Baron's wings have a 80 gallon capacity. The weight of this fuel exceeds that of the wing being tested by a factor of 2.6. Tests designed to evaluate the influence of the fuel on the interior pressure were performed using lead shot bags and 5-10 pound blocks of sand wrapped in plastic bags to simulate the mass fuel mass. The total weight added of 217 pounds approximately equals the weight of the wing. It was distributed evenly inside the leading edge of the inboard fuel tank, this tank extending outboard from the wing root approximately 100 inches. As in the previous test, the level of the airborne flanking path was estimated by comparing the results of tests performed with the wing attached to the fuselage and with it totally detached. The difference in cabin pressure for a force excitation of the engine mount is shown on Fig. 10. When compared with Fig. 8 these results give slightly smaller differences (e.g., 2 dB) in the frequency range above 150 Hz.

The changes relative to the standard configuration (Figs. 6) in interior pressure for various excitation locations due to the presence of the fuel mass are shown on Figs. 11. Above 60 Hz the presence of the mass reduces the cabin pressure levels by approximately 15 dB for all excitation locations but 26 (wing skin outboard of engine mount). The reason for this latter result is not known; however, this location is adjacent to damaged wing skin.

3. Interior Acoustic Volume Absorption

Forces applied to the wing are transferred to the structure of the fuselage through the bolted connection. These loads in turn excite vibrations in the fuselage and an acoustic field within the cabin. Sound radiation can be associated with both the near field of the vibrational response of the fuselage which would be localized near the wing connection and with the propagating vibrational field (i.e., the far field) that carries energy along the fuselage. As a diagnostic means of separating these contributions, the forward portion of the cabin between the wing connection and the microphone location (i.e., approximately a six foot length of the cabin forward of the rear seats) was filled with acoustically absorbing foam.

The intent of this test was to preferentially add acoustic absorption to the path of the nearfield radiation from the structural region near the wing interface.

The result of this test is shown on Fig. 12 as the difference in the interior pressure level between the standard test configuration and that having the foam inserted. In both configurations the wing is attached to the fuselage and the excitation location is the engine mount. Little effect of the foam is found throughout the frequency range, although a slightly increasing trend is observed above the frequency noted by the arrow for which the spatial extent of the added foam measures an acoustic wavelength. Increased performance in this frequency range would be expected for an acoustic path through the foam acting as a volume absorber; however, the small effect measured suggests that the sound induced by the vibrational field of the fuselage away from the location of the wing connection is an important contributor to the interior noise field.

IV. CONCLUSIONS

Analysis of the data obtained from the tests on the Beechcraft Baron leads to the following conclusions regarding the structureborne propagation path:

1. In the frequency range below 400 Hz substantially higher cabin pressures are obtained when a unit force is applied to the wing structure than when applied to the fuselage at a wing mounting bolt location. Differences of up to 30 dB are obtained in the frequency range corresponding to fundamental resonances of the wing (i.e., 30-40 Hz). This suggests that wing excitation provides a more efficient coupling mechanism to the vibrational modes of the fuselage than provided by a localized force excitation of the fuselage.

2. When the wing is disconnected from the fuselage, the acoustic pressure level in the cabin is down approximately 15 dB below that obtained with the wing attached. This is interpreted to mean that the flanking path associated with radiation through the air of wing vibrational energy is only down by 15 dB.

The airborne path would be reduced by sidewall treatment designed to reduce acoustic transmission into the cabin. The effect of the -15 dB flanking path is to increase the difficulty of experimentally verifying means to reduce the structureborne path by more than this amount. For example measured noise reduction due to a compliant connection between the wing and fuselage would at best be 15 dB. Diagnosis of this flanking path during structureborne noise tests would be more difficult for aircraft having non-bolted wing connections.

3. The addition of 217 pounds of simulated fuel into the leading edge tanks of the wing reduces the pressure in the cabin per force excitation by approximately 15 dB. It is assumed that the presence of this mass directly reduces the force transmitted to the fuselage. It follows that the contribution to the cabin noise due to the structureborne path increases throughout a flight as fuel is consumed.

4. Added acoustic absorption in the cabin volume only begins to be effective in reducing cabin noise when its thickness is comparable with an acoustic wavelength. The relatively small effect of the volume absorption on the measured sound pressure suggests that the interior noise is not dominated by radiation from the structural near fields at the interface of the fuselage with the wing.

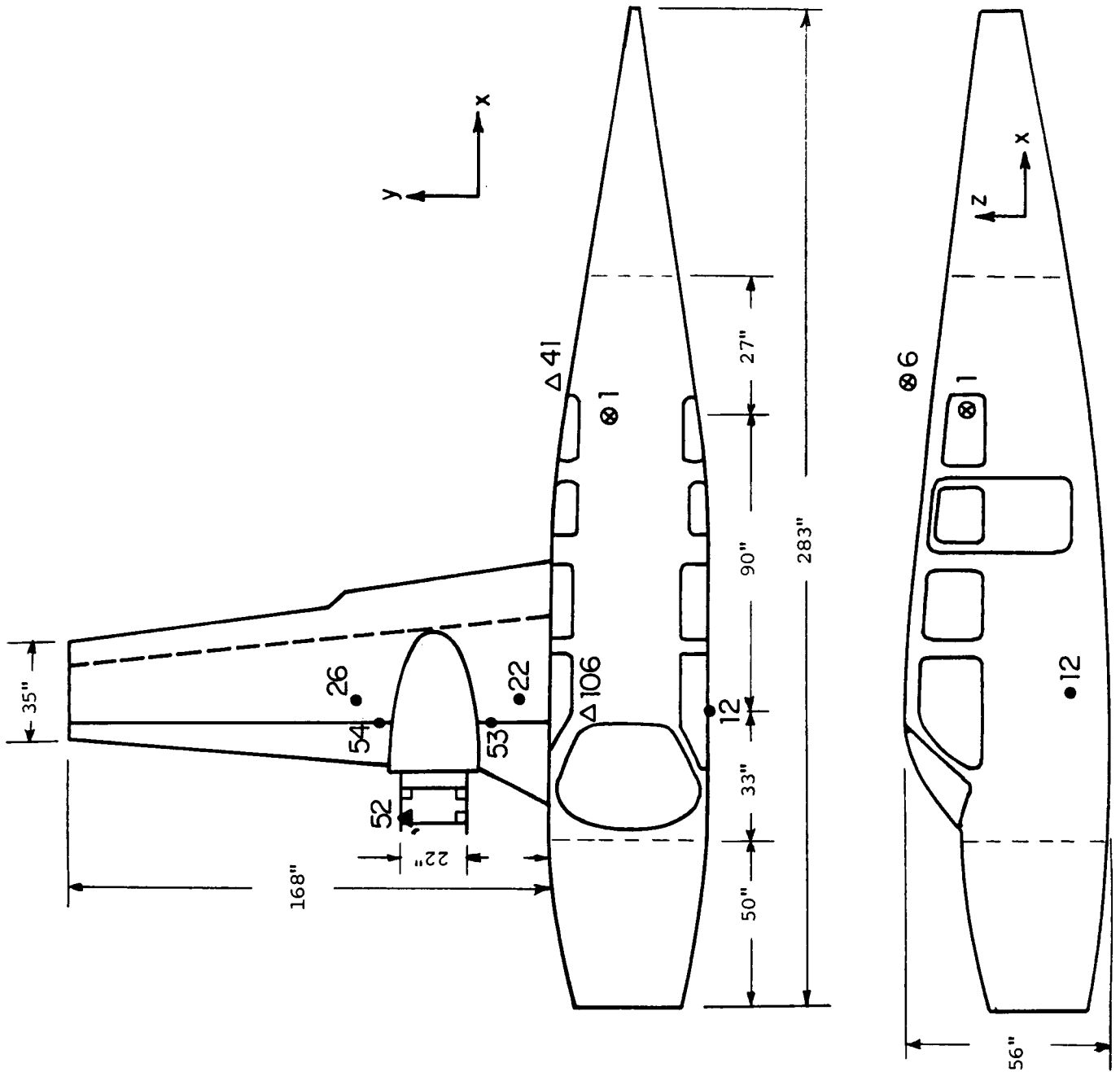


Fig. 1 Aircraft geometry and locations of hammer excitation (o), microphones (⊠), and accelerometers (Δ).

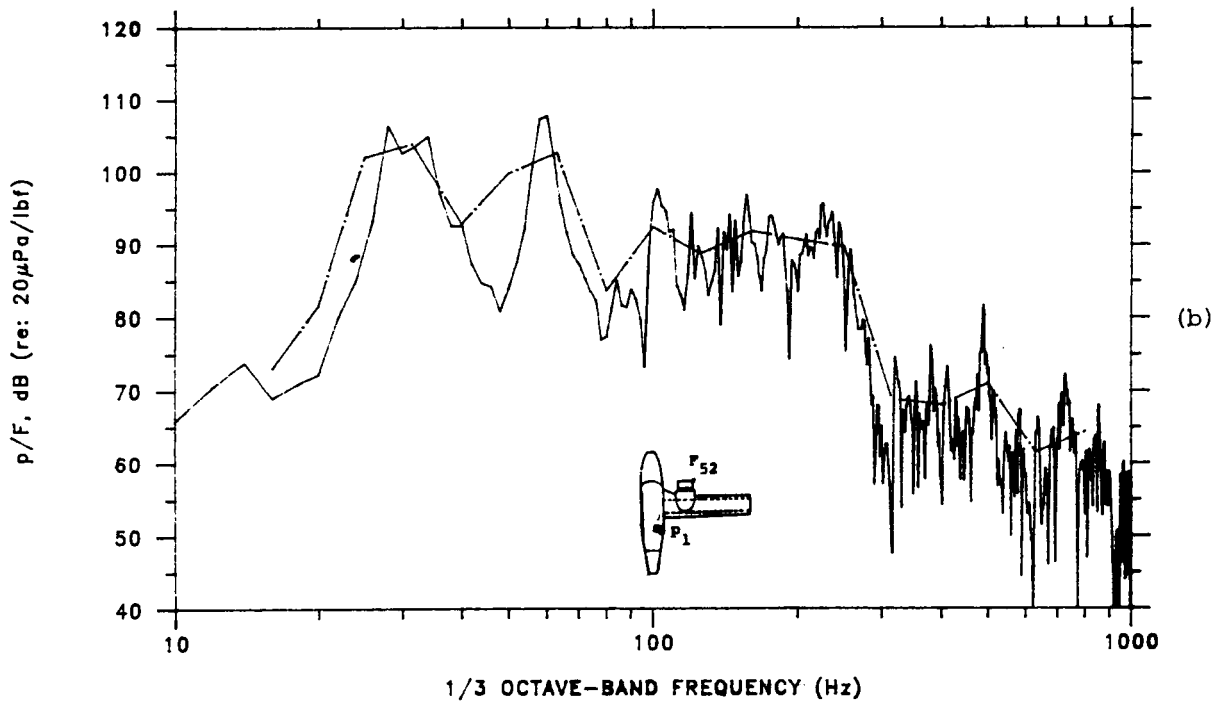
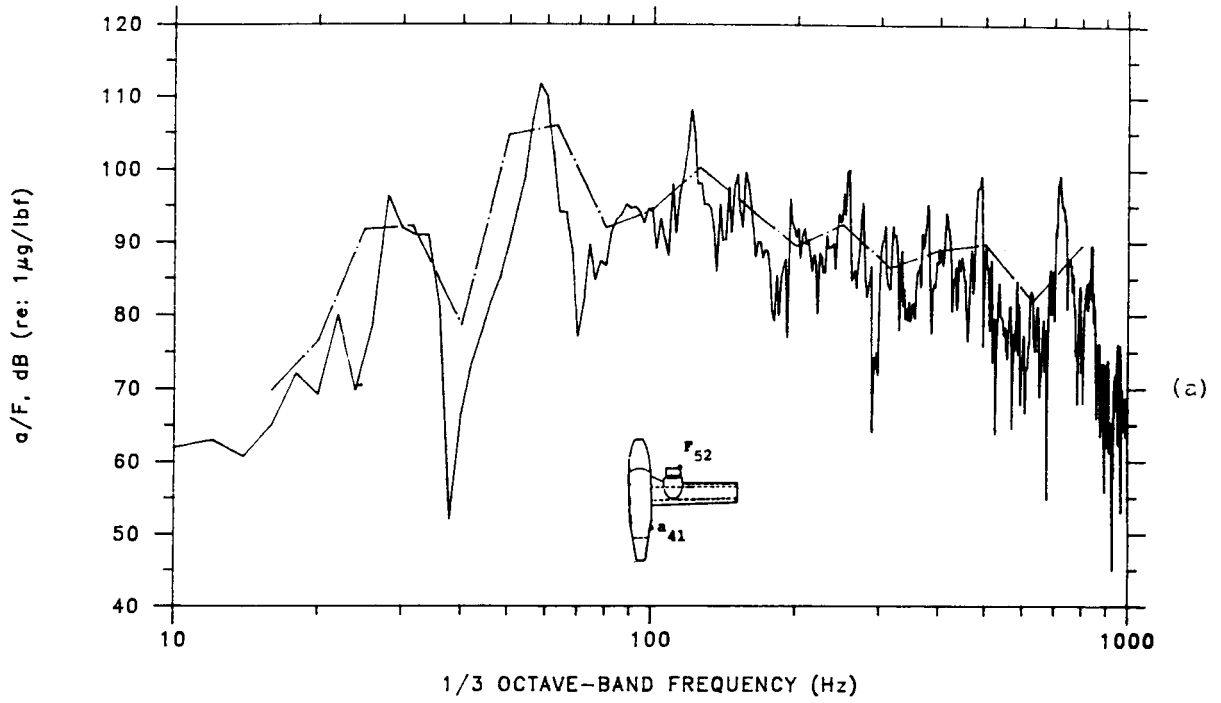


Fig.2a Comparison of transfer function between (a) cabin sound pressure and (b) fuselage acceleration and force applied to the wing engine mount in frequency bandwidths of 2 Hz (—) and $1/3$ octave band (---).

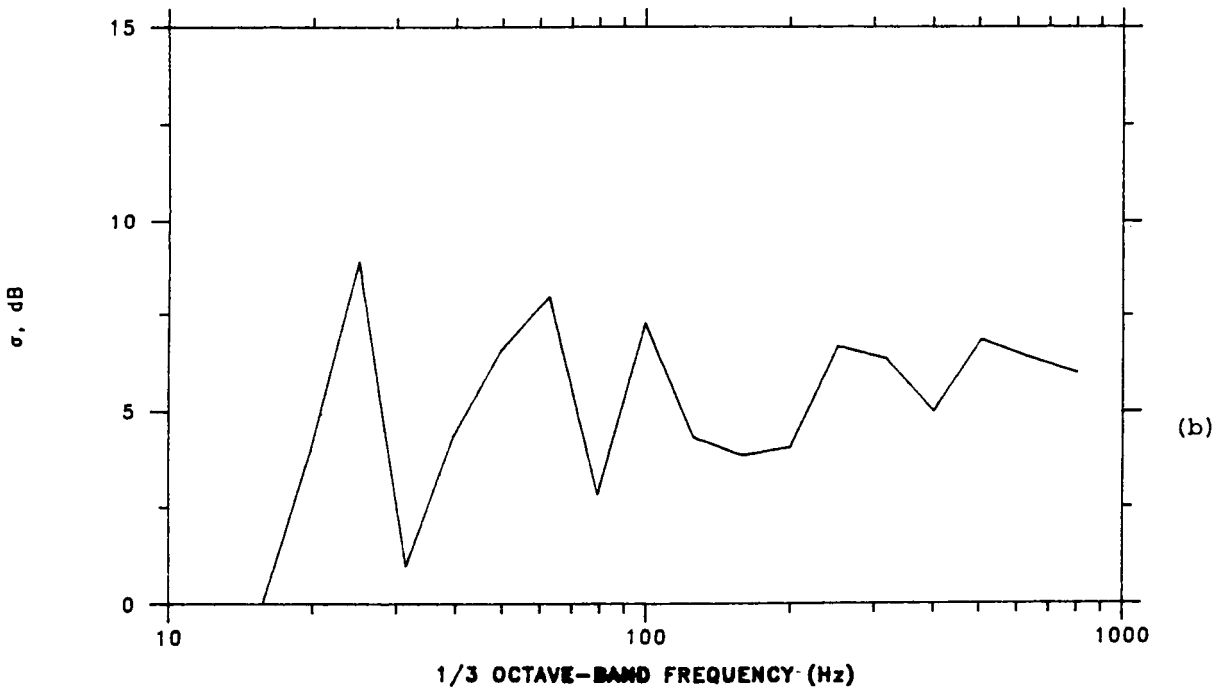
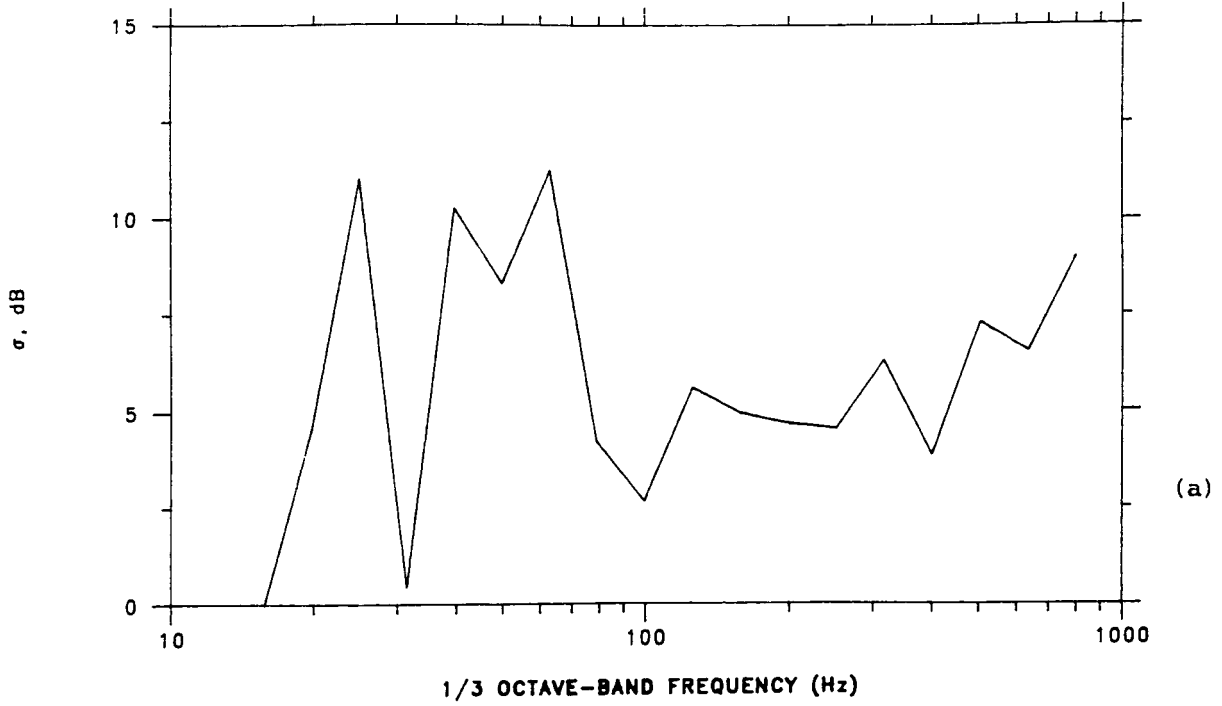
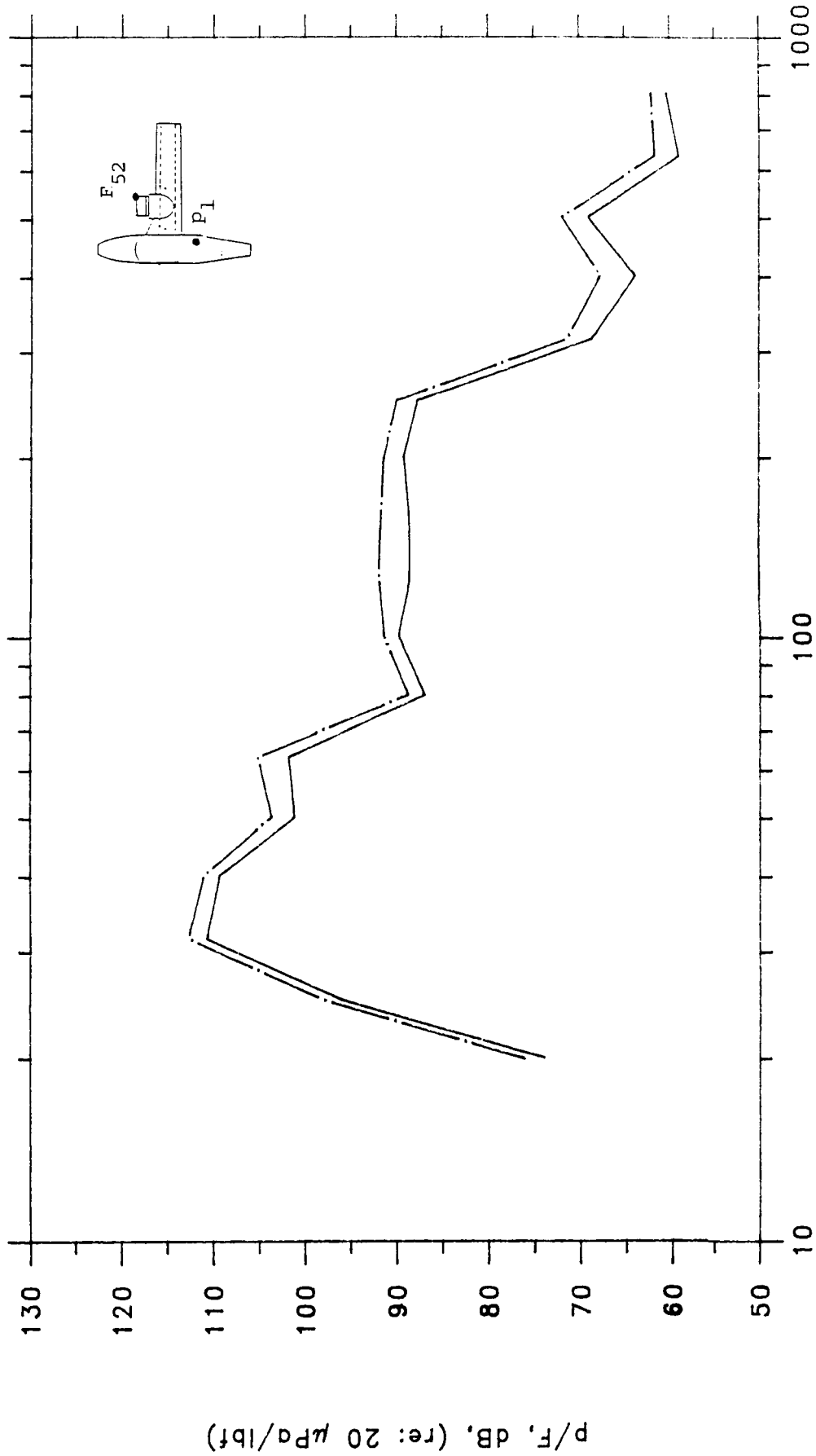


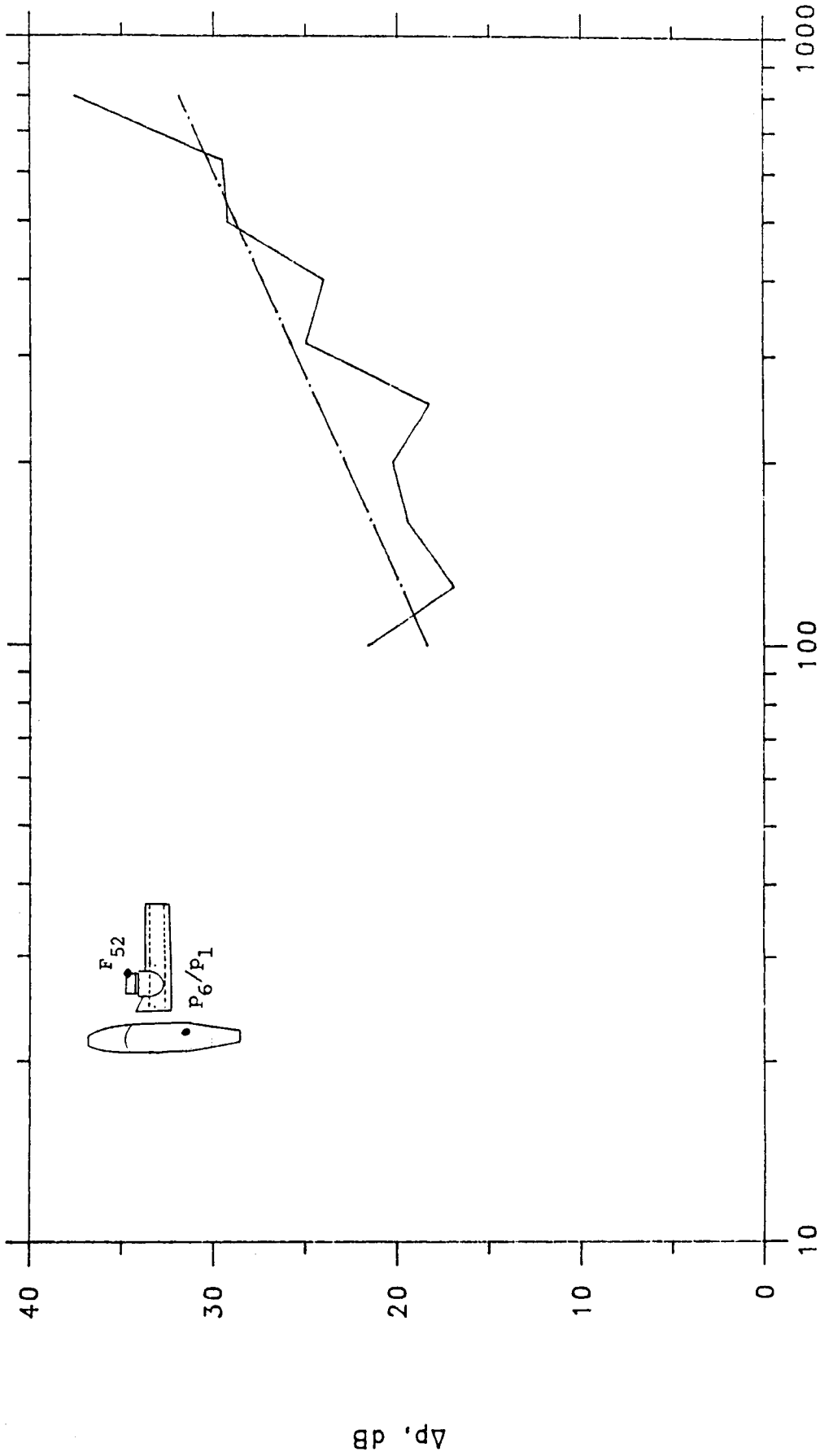
Fig. 2b Standard deviation of narrowband levels within each 1/3-octave band for the corresponding transfer functions shown in Fig. 2a.



1/3 OCTAVE-BAND FREQUENCY (Hz)

Fig. 3 Comparison of transfer function between cabin sound pressure and force applied to the wing engine mount during two separate tests of the standard wing configuration.

DIFFERENCE



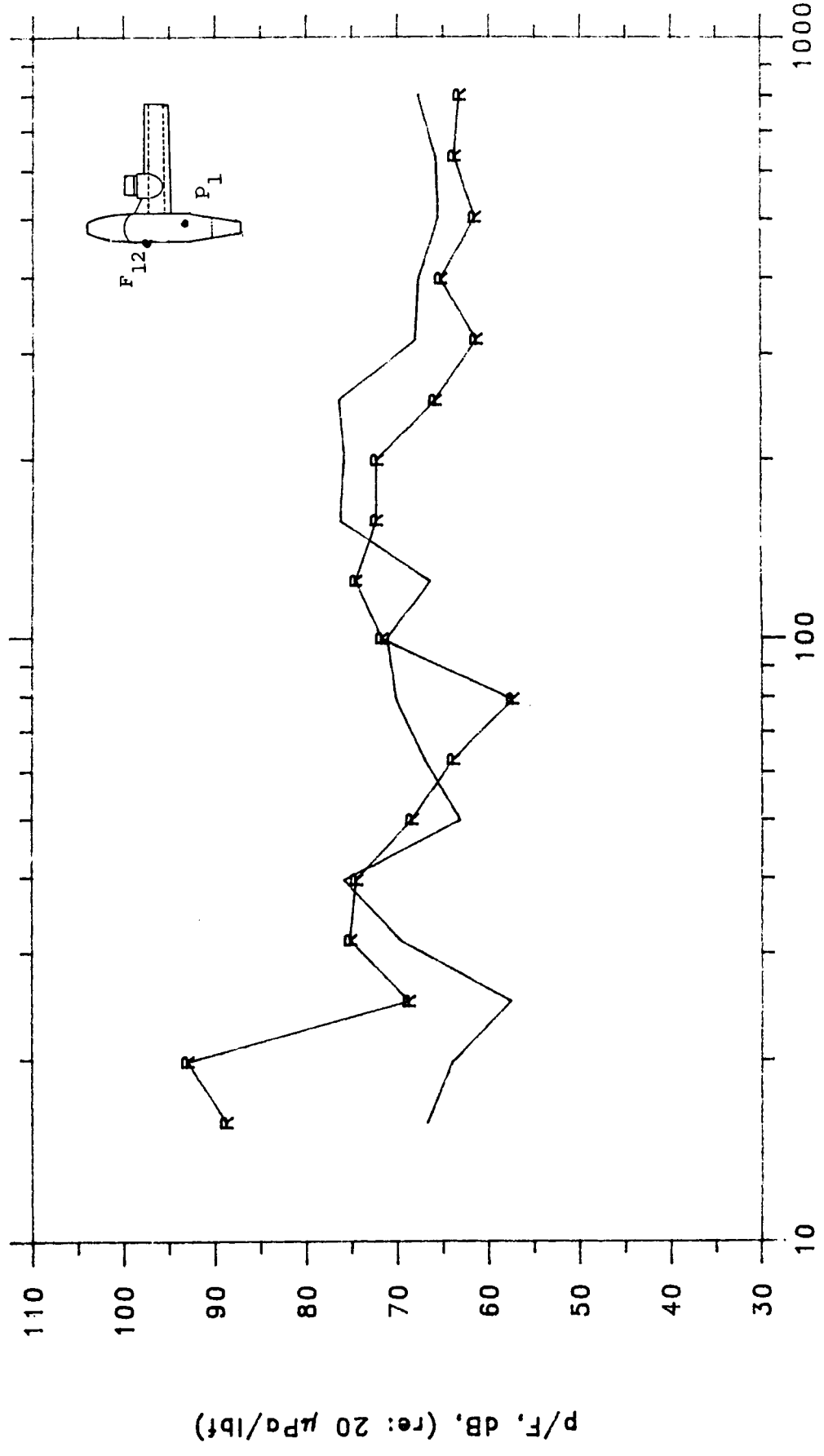
1/3 OCTAVE-BAND FREQUENCY (Hz)

Fig. 4 Comparison of measured fuselage noise reduction with random incidence acoustic transmission loss for an aluminum panel of thickness 0.033 inches.

CAA, Inc.

TRANSFER FUNCTION

RMS AVERAGE
CAATF315&CAATF410
CAATF2B.RECIPROCAL



1/3 OCTAVE-BAND FREQUENCY (Hz)

Fig. 5a Comparison of transfer functions between the cabin pressure at location 1 and the fuselage top forward wing attachment bolt (location 12). (—, direct method; - - -, reciprocal method.)

TRANSFER FUNCTION

RMS AVERAGE
CAATF310 & CAATF311
CAATF417, RECIPROCAL

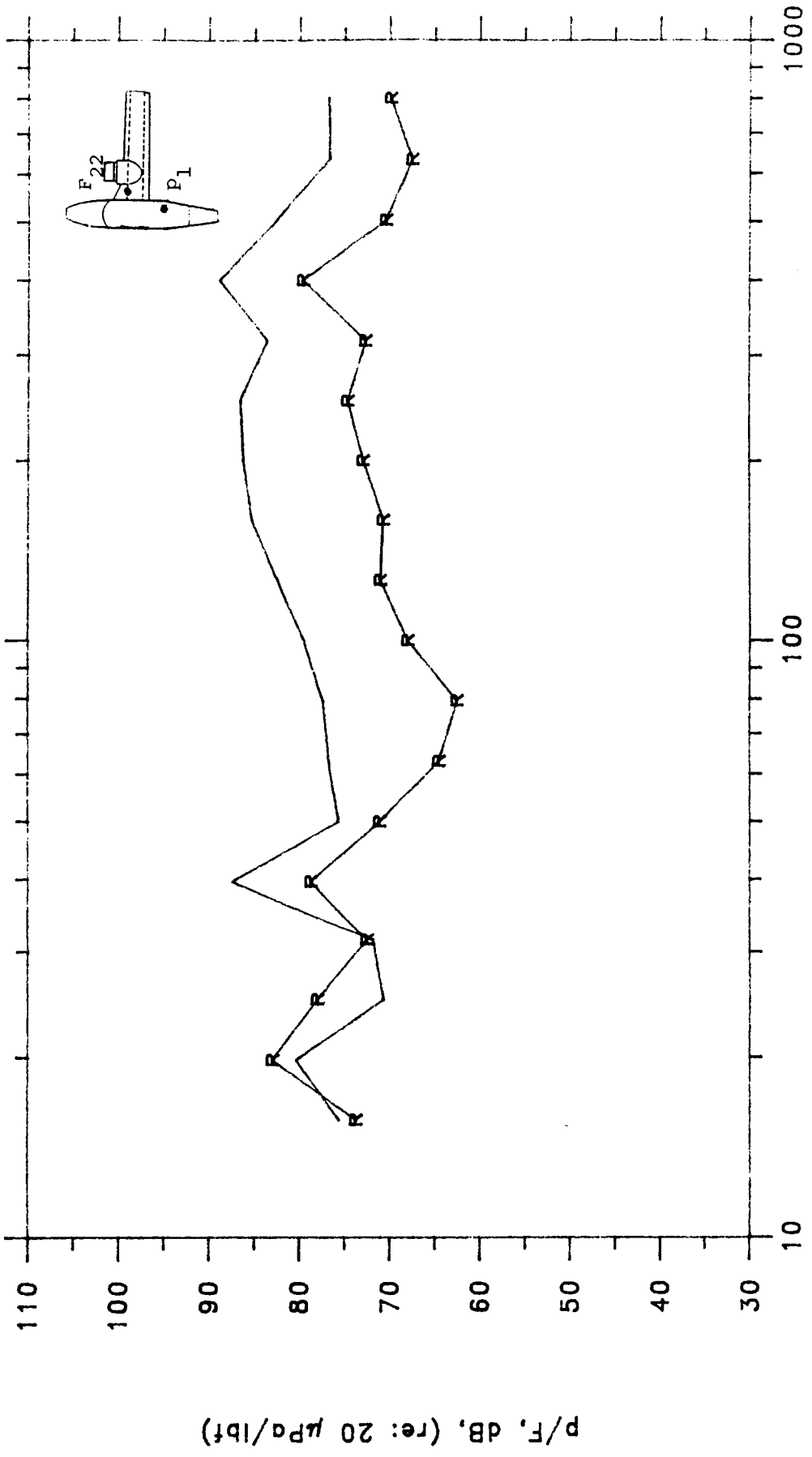
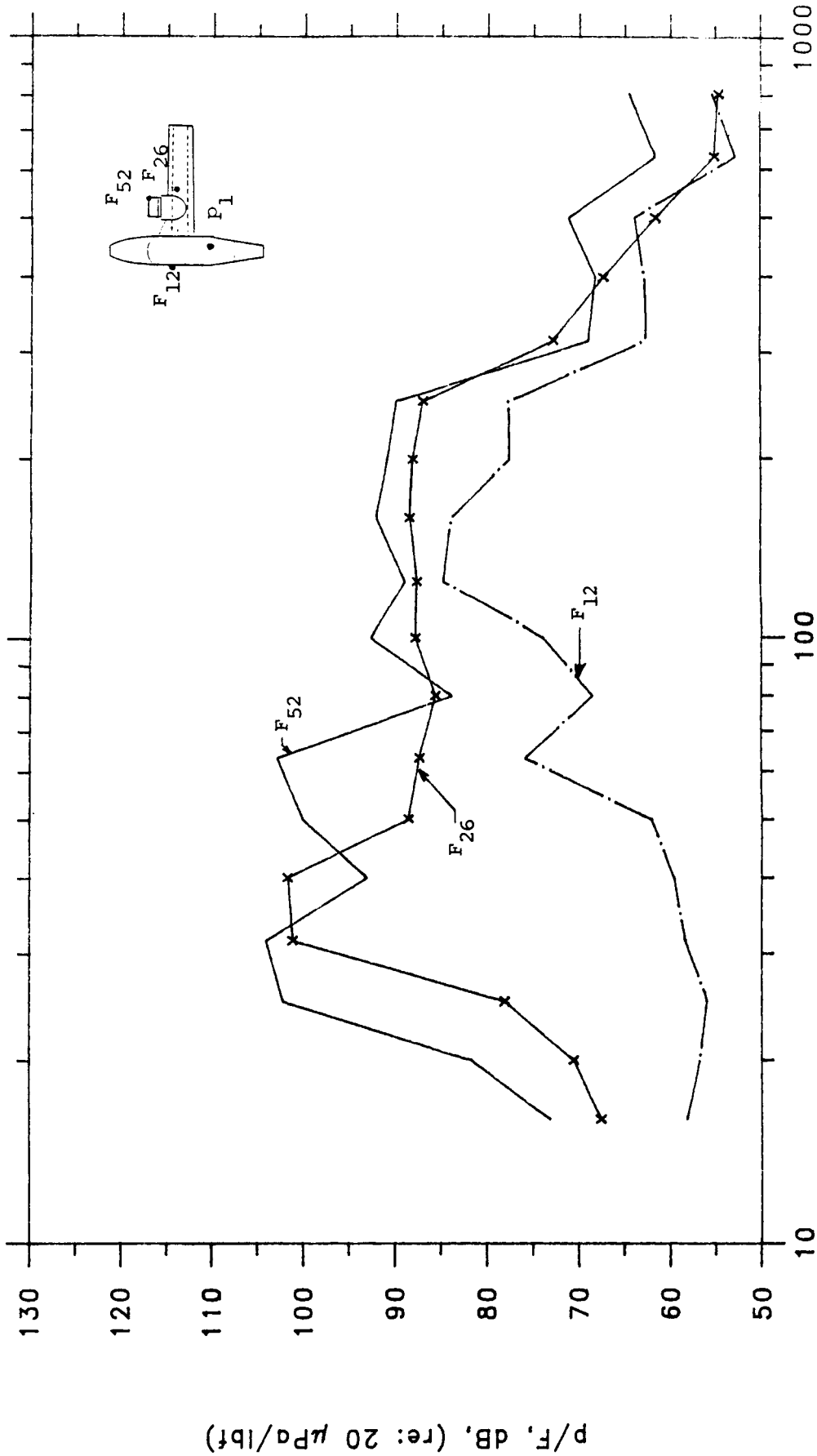


Fig. 5b Comparison of transfer functions between the cabin pressure at location 1 and the inboard wing skin (location 22) (—, direct method; —R—, reciprocal method).



1/3 OCTAVE-BAND FREQUENCY (Hz)

Fig. 6a Transfer function between cabin sound pressure and force applied to various locations on the wing and fuselage for the standard wing configuration.

TRANSFER FUNCTION

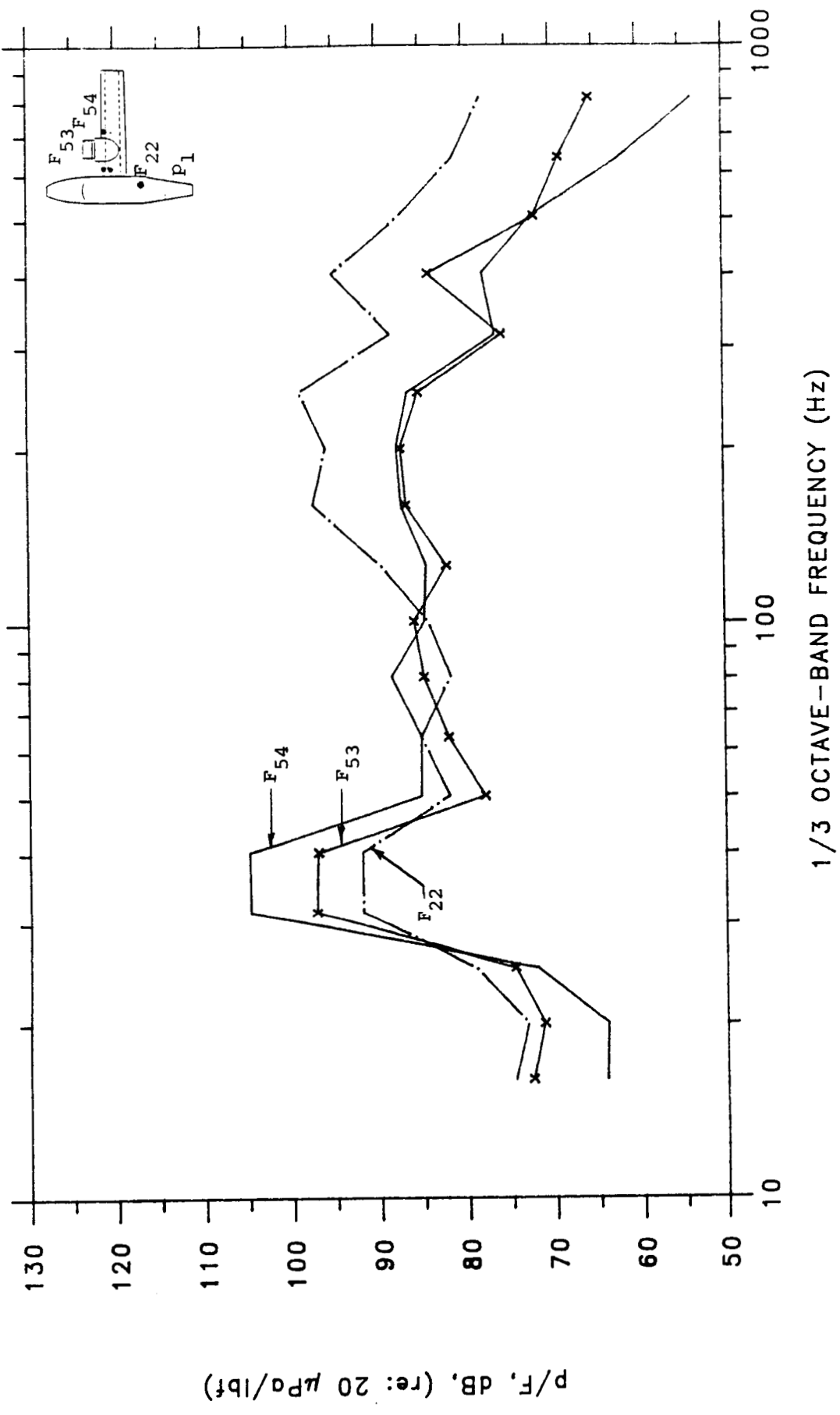
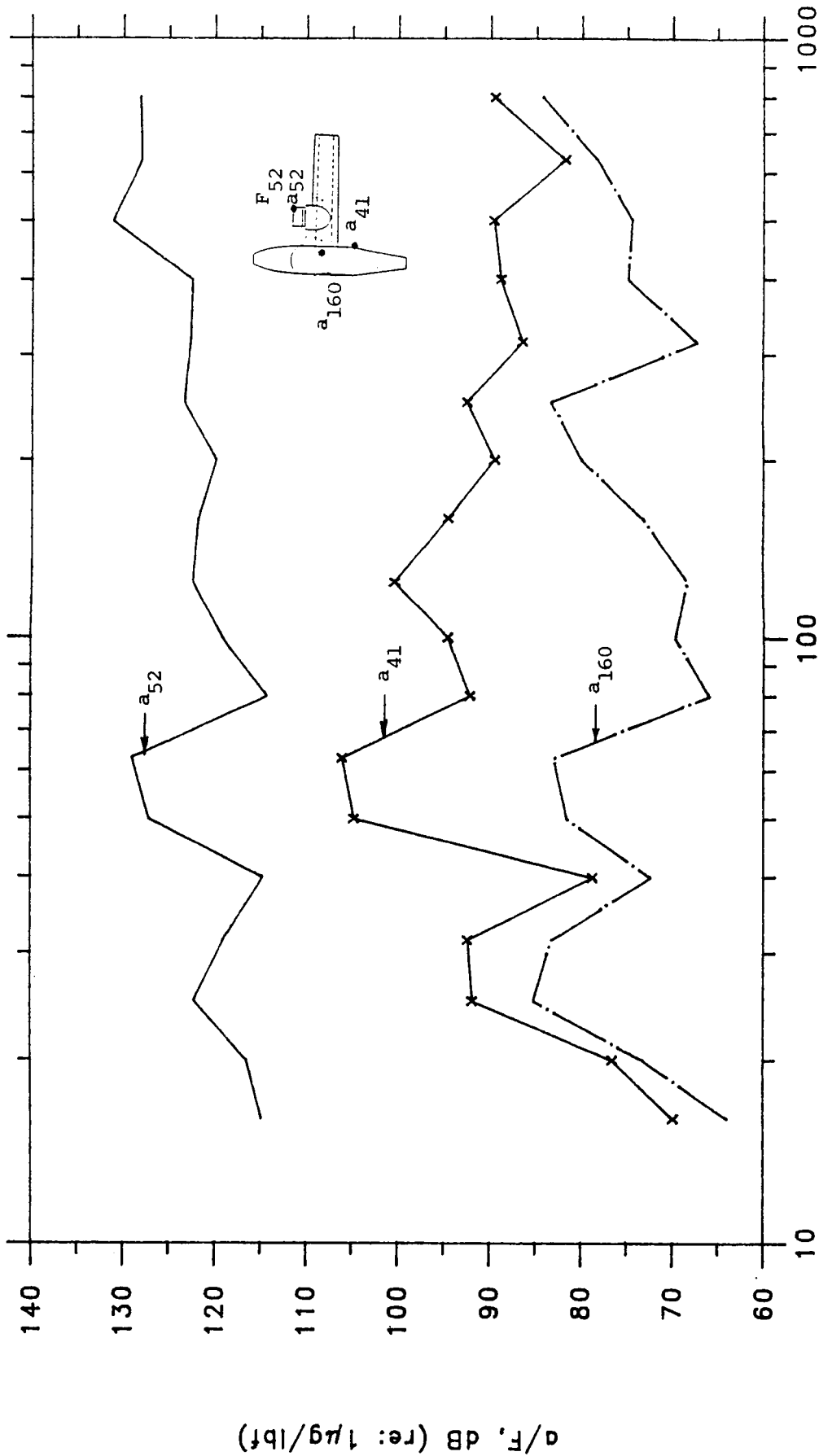


Fig. 6b Transfer function between cabin sound pressure and force applied to various locations on the wing and fuselage for the standard wing configuration.

CAA, Inc.

TRANSFER FUNCTION

— CAA215.PRN
- - CAA62.PRN
x CAA213.PRN



1/3 OCTAVE-BAND FREQUENCY (Hz)

Fig. 7a Comparison of the transfer function between acceleration at several locations and force applied to the wing engine mount with the standard wing configuration.

DRIVE POINT RESPONSE

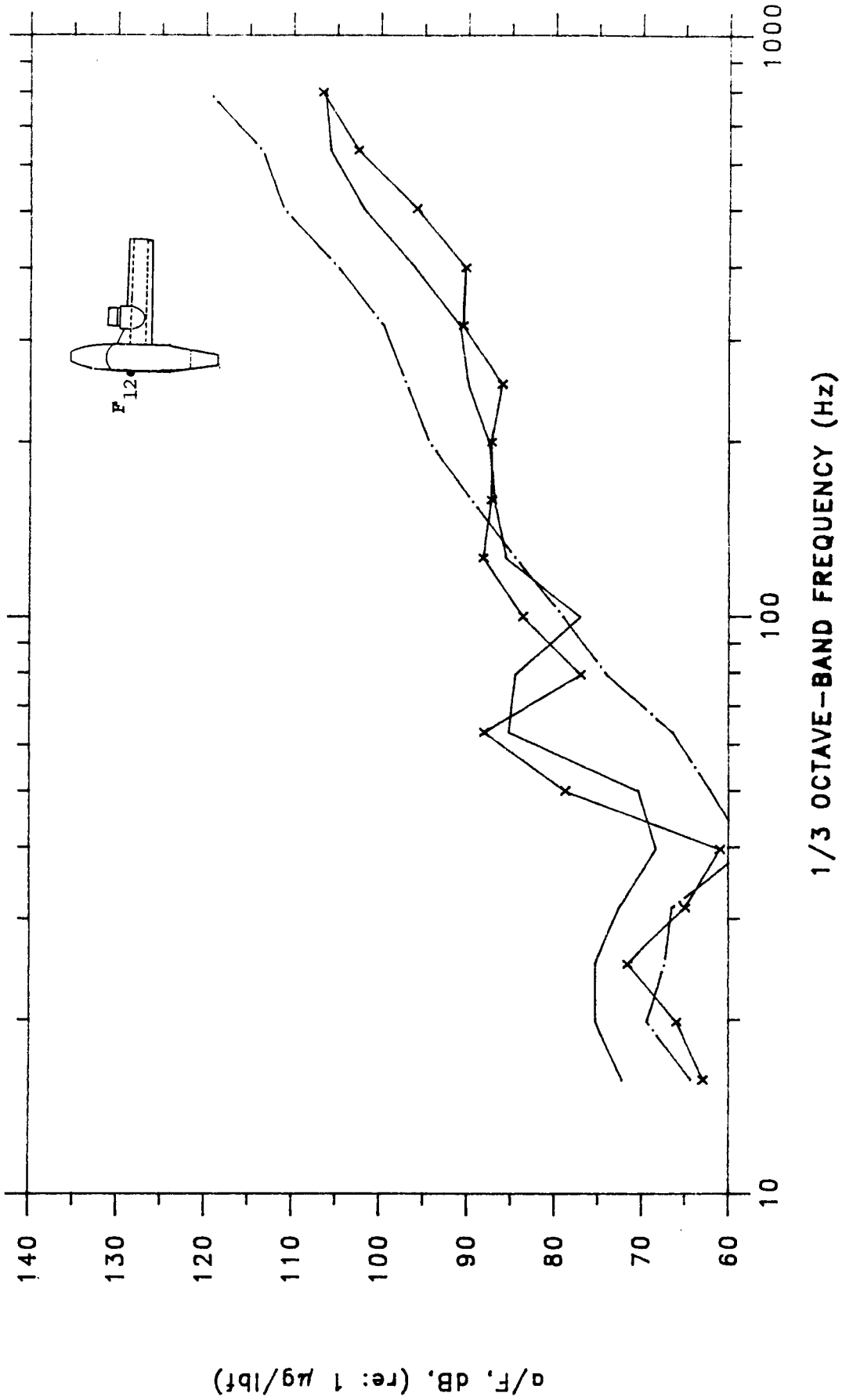
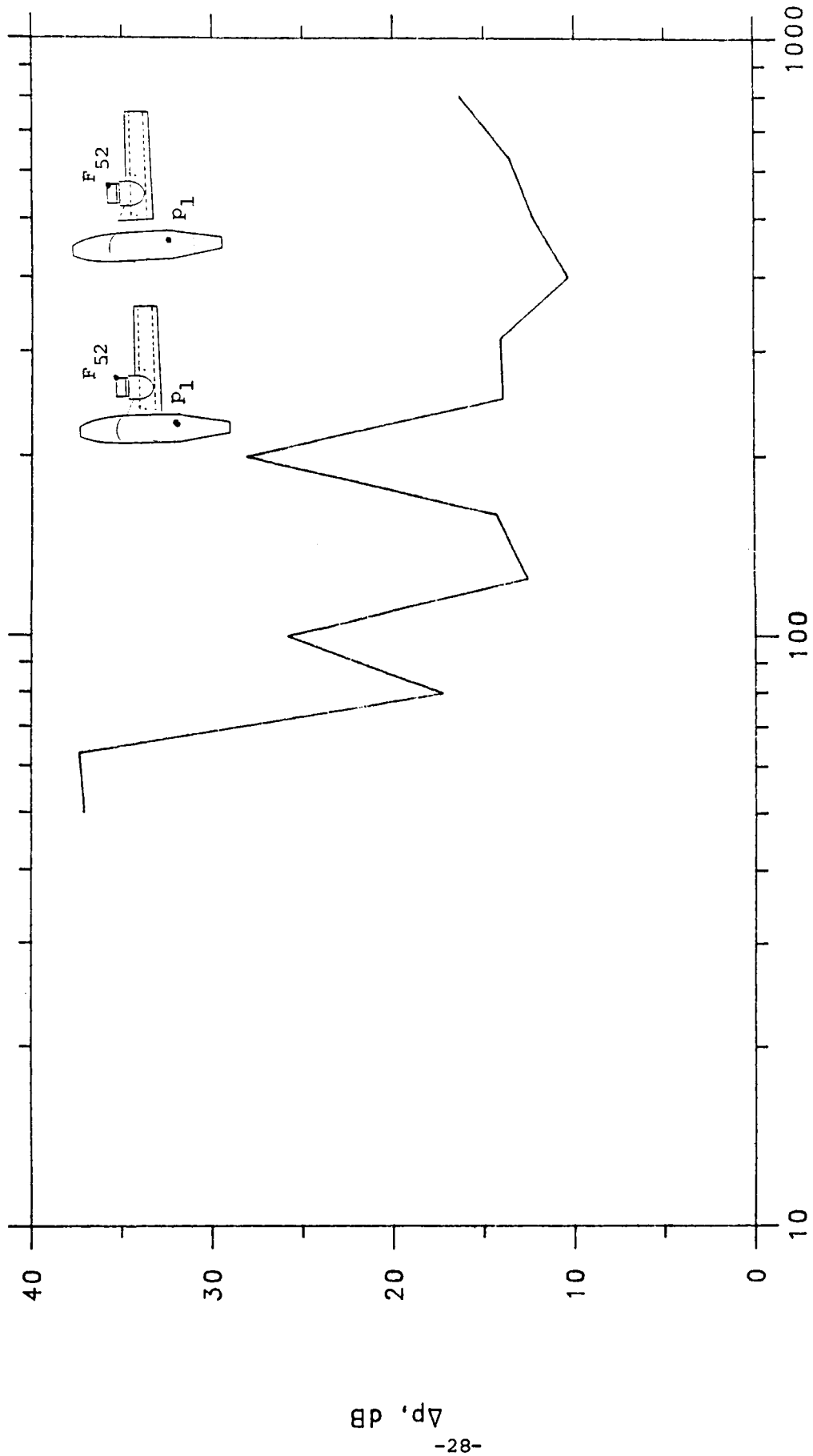


Fig. 7b Drive point acceleration at the fuselage top forward wing attachment bolt (location 12) in the lift (—), thrust (---), and span (X—X—) directions.

DIFFERENCE



1/3 OCTAVE-BAND FREQUENCY (Hz)

Fig. 8 Difference between cabin sound pressures excited by a force applied to the wing engine mount with and without the wing (in its standard configuration) attached.

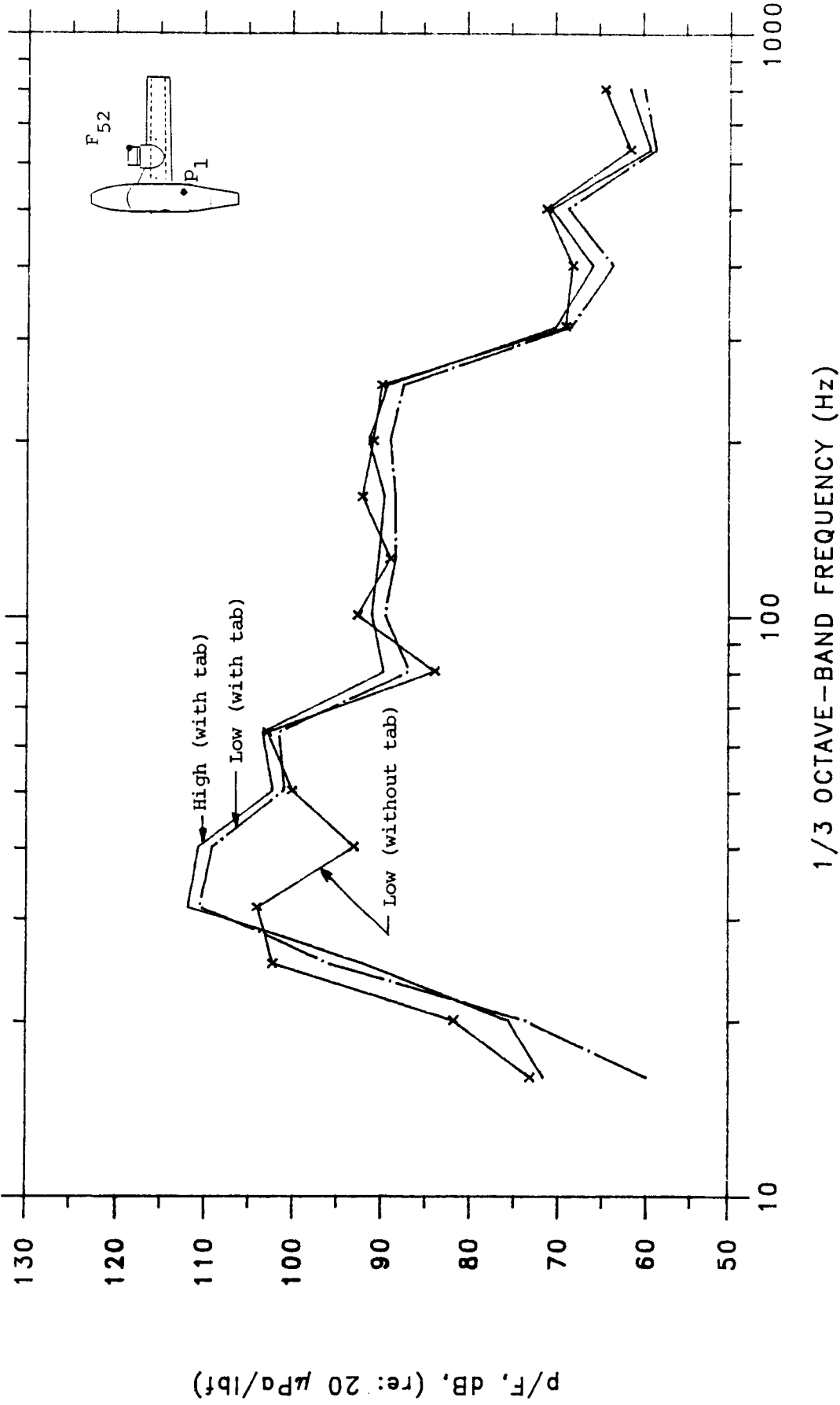
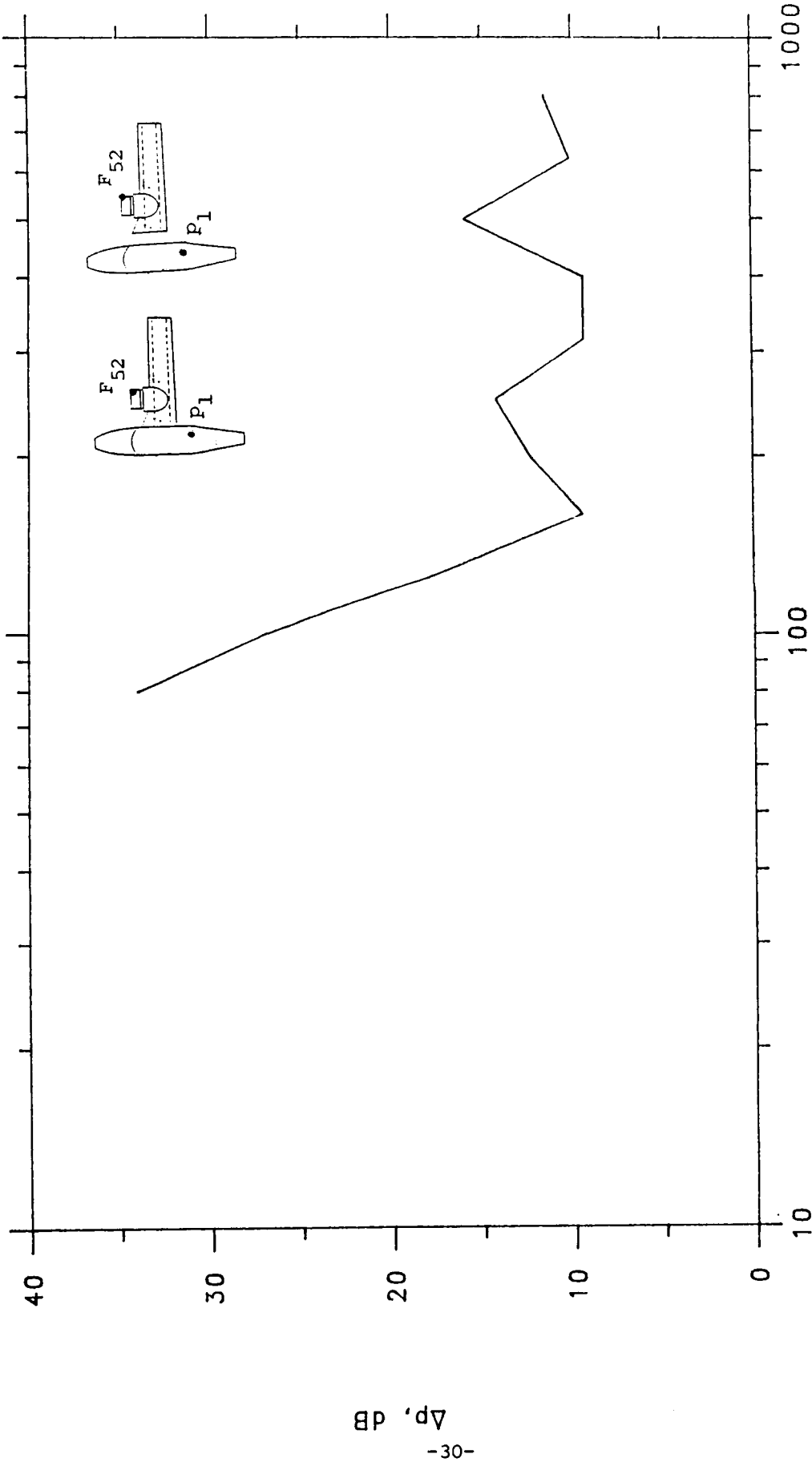


Fig. 9 Comparison of the transfer function between cabin sound pressure and force applied to the wing engine mount with different bolt numbers and torque.

DIFFERENCE

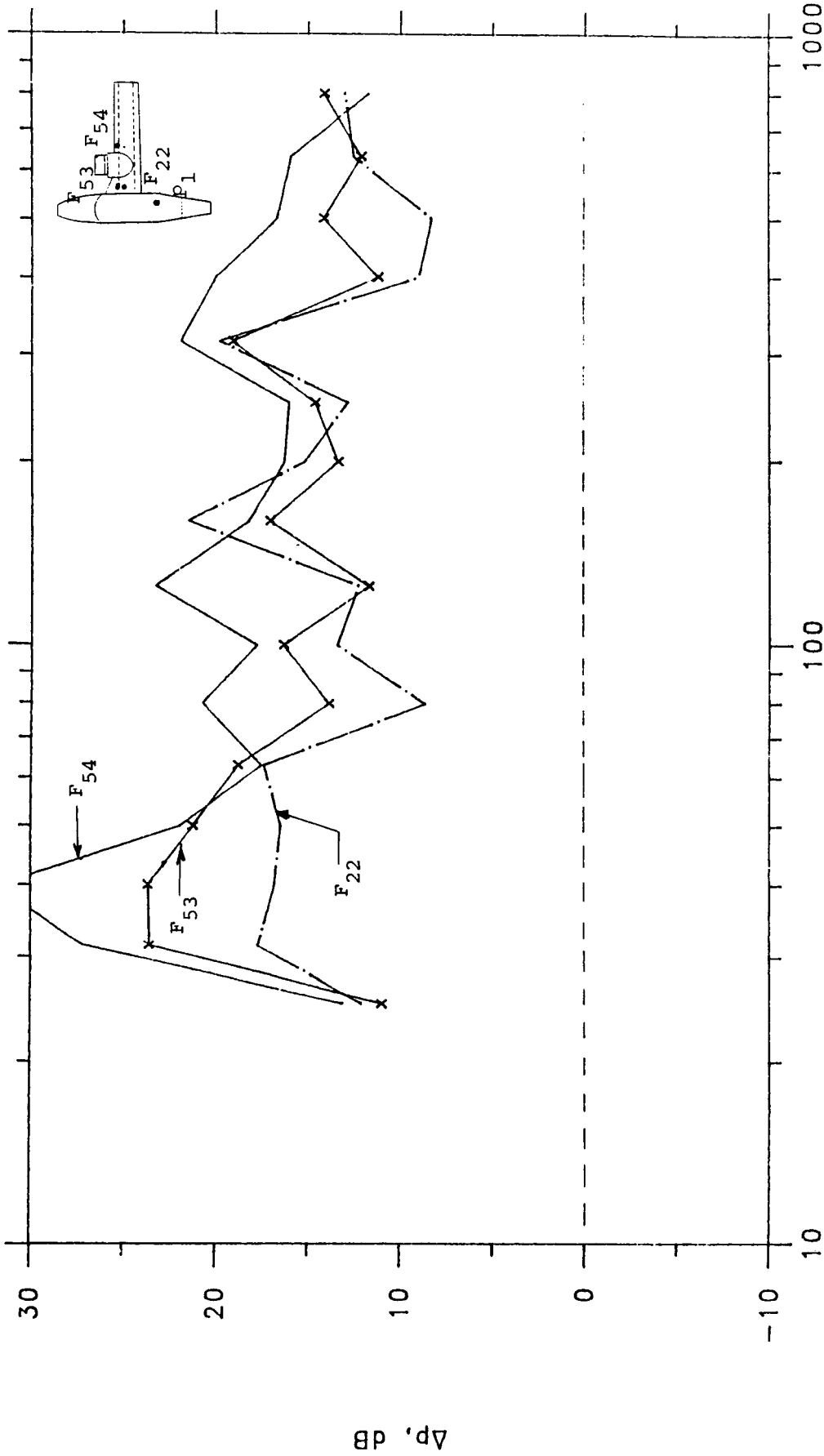


1/3 OCTAVE-BAND FREQUENCY (Hz)

Fig. 10 Difference between cabin sound pressures excited by a force applied to the wing engine mount with and without the (mass-loaded) wing attached.

— CAA221.PRN-CAA415.PRN
 - - - CAA222.PRN-CAA417.PRN
 * CAA223.PRN-CAA416.PRN

DIFFERENCE

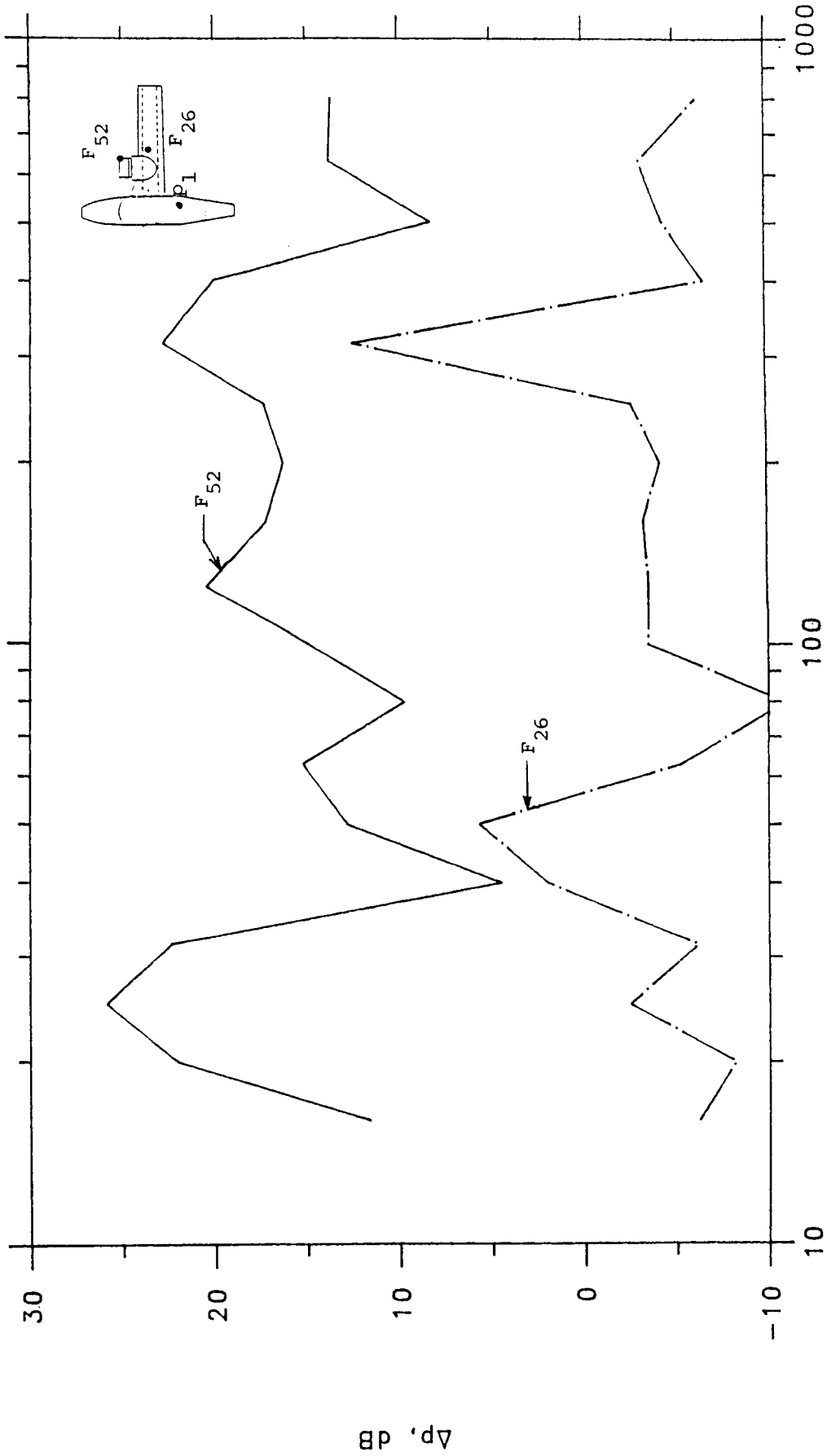


1/3 OCTAVE-BAND FREQUENCY (Hz)

Fig. 11a Difference between cabin sound pressures excited by a force applied at various points on the wing without and with the wing mass loading.

CAA216.PRN - CAA410.PRN
CAA220.PRN - CAA414.PRN

DIFFERENCE



1/3 OCTAVE-BAND FREQUENCY (Hz)

Fig. 11b Difference between cabin sound pressures excited by a force applied at various points on the wing without and with the wing mass loading.

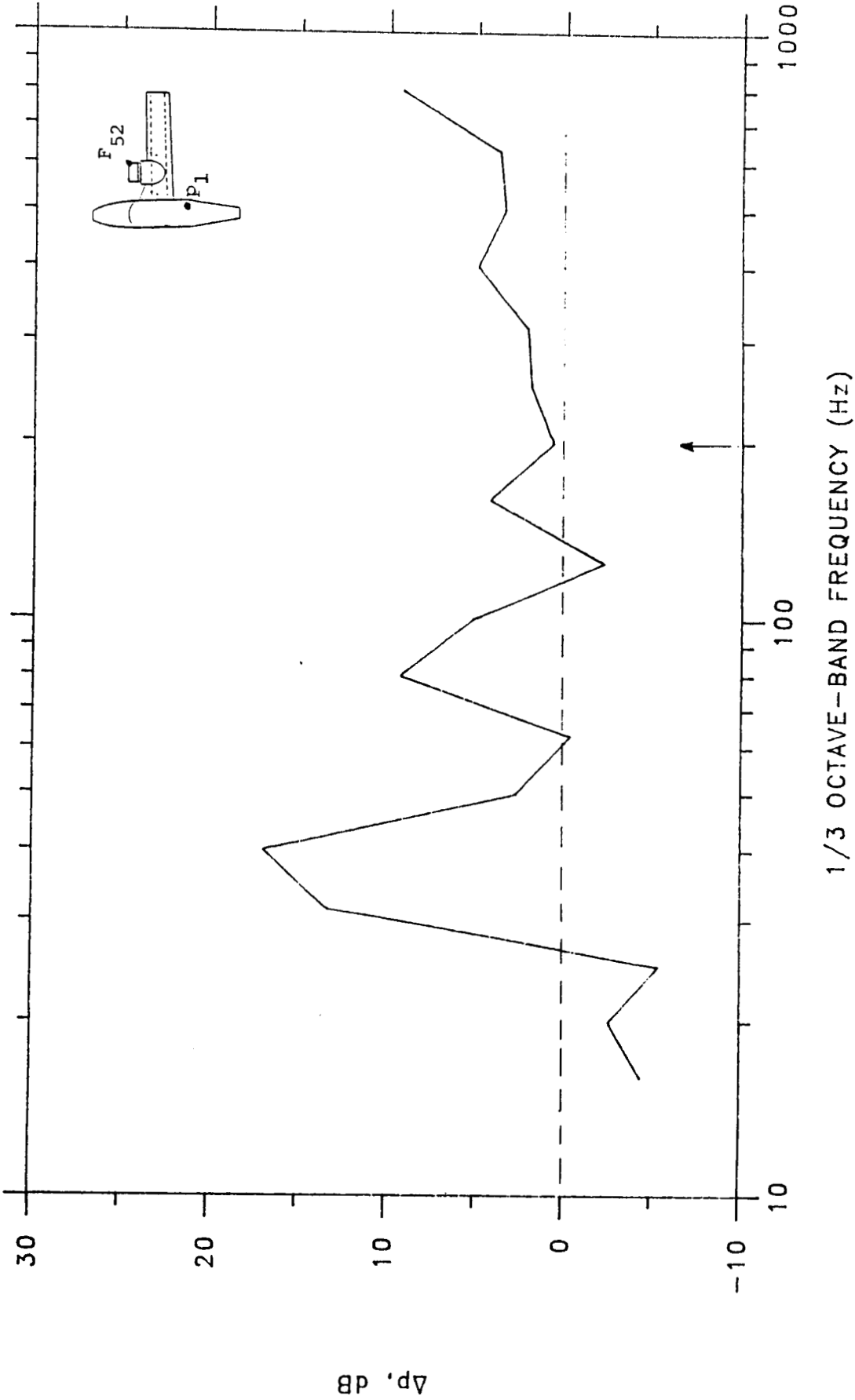


Fig. 14. Difference between cabin sound pressures excited by a force applied to the wing engine mount without and with added acoustic absorption in the cabin. (Arrow indicates frequency whose wavelength measures the length of treated cabin.)

REFERENCES

- 1 L.E. Kinsler and A.R. Frey, Fundamentals of Acoustics (John Wiley and Sons, NY, 1962) p. 140.
- 2 Ten Wolde, Reciprocity Experiments on the Transmission of Sound in Ships, (Drukkerij Hoogland en Waltman, N.V., Delft, the Netherlands, 1973) 16-17.

APPENDIX A

MODAL TEST EVALUATION OF LOW FREQUENCY WING DYNAMICS

APPENDIX A

MODAL TEST EVALUATION OF LOW FREQUENCY WING DYNAMICS

A.I INTRODUCTION

The low frequency dynamics of the wing were evaluated during the weeks of November 17, 1986 and April 2, 1987 using experimental modal analysis. Tests were performed on the right-hand wing in several configurations including (1) freely-supported with and without the attached engine mount and (2) attached to the fuselage. Some comparison tests were also performed on the left-hand wing.

The purpose of these tests was to determine the lower order mode shapes and resonance frequencies of the wing when excited in the lift direction. This information provided guidance for the development of the finite element model of the wing.

A.II PROCEDURE

In the freely-supported configuration the wing rests on several air-filled rubber tubes distributed along the span of the wing. Excitation of the wing is by means of a 4 ounce hammer instrumented with a force gauge. Transfer accelerances are measured reciprocally by exciting the wing at ten locations along the forward and aft spars of the wing and measuring the acceleration response using a Bruel and Kjaer 4332 accelerometer located midway between points 160 and 170 on the forward spar (see Fig. A-1). This procedure makes use of the existence of reciprocity between excitation and response locations on the structure. As discussed in Section III.B of this report, however, reciprocity requires perfect coherence between excitation and response signals. In general this requirement is not satisfied in the testing. Regions of low coherence exist at low frequency and in the region of antiresonances. High coherence (greater than 0.90) however is found in the vicinity of strong resonances, these regions being more important to the experimental determination of mode shapes.

Data are acquired and analyzed using the GenRad 2515 Computer Aided Test System. Because the emphasis is on the fundamental vibrational modes of the wing, the upper frequency limit is set for 148 Hz. Resonances of the wing skin vibrating between stiffeners begin to occur around 200 Hz and therefore are not present in the data collected for modal analysis. Data acquisition uses a frequency bandwidth of 0.5 Hz.

The transfer accelerance (i.e., the acceleration normalized by the excitation force) is computed for each excitation location. Results of ten hammer impacts are averaged to obtain each transfer function.

Computation of resonance frequencies, mode shapes, and modal damping is performed by means of the Modal-Plus software package of Structural Dynamics Research Corporation. The algorithm used in this package fits the response function of a multiple degree-of-freedom linear system to the measured transfer functions. Effects of non-linearities or noise in the measurements can result in the computation of so-called "fictitious" structural modes. One discriminator used in recognizing these modes is the modal loss factor. In general the fictitious modes have unrealistically high values of modal damping. Modes having loss factors greater than 0.25 are therefore not considered to be valid modes of the structure and are eliminated from the final curve fit and data analysis.

A.III RESULTS

A. Freely-Supported Wing

Nine vibrational modes of the wing are computed in the frequency range below 148 Hz for the freely-supported wing without the engine mount while ten modes are obtained in the same frequency range when the engine mount is attached. A representative comparison between a measured transfer function and the curve fit to the data computed by the Modal-Plus software is shown on Fig. A-2. The fit of the curve to the measurements is found to be best in those regions where the measured response is highest (i.e., near resonances).

The resonance frequencies and modal loss factors for the freely-supported wing with and without the presence of the engine mount are listed in Table A-I. Corresponding mode shapes are shown in Appendices B and C. For both configurations the fundamental bending and torsional modes occur near 45 and 53 Hz, respectively. The influence of the engine mount is more clearly seen in the results above 100 Hz.

B. Wing Attached to Fuselage

In this configuration the wing with attached engine mount is bolted to the fuselage using a torque of 50 foot-pounds. Both the fuselage and the tip of the wing are softly supported using the air-filled tubes. The fundamental resonance frequency of the attached wing acting as a cantilever beam is found to be less than 10 Hz. Clear definition of the lower order modes of the attached wing is made difficult because of both the relatively low excitation provided by the hammer in this frequency range and the 0.5 Hz analyzer bandwidth.

The resonance frequencies and modal loss factors determined for this configuration are listed on Table A-II. Mode shapes obtained for this configuration are given in Appendix D (with the exception of modes 2 and 3). The fundamental mode at 3.8 Hz is primarily the rigid-body rotation of the wing due to the elastic support of the fuselage. Based on the stiffness of the freely supported wing, the true cantilever mode of the wing would occur at approximately 7 Hz.

C. Parameter Sensitivity

1. Force Amplitude

During the testing performed in April 1987, several parameters were varied to examine the sensitivity of the wing dynamics. Shown on Fig. A-3 are the transfer functions between the same locations on the right wing with different force levels. The force in the results of Fig. A-3b is approximately 10 times that of the results in Fig. A-3a, this increase being achieved through a harder hammer impact rather than a change in hammer tip. This increase in

excitation produces substantially higher coherence between the excitation and the response in the frequency range below 150 Hz. The increased force amplitude has little effect on the measured transfer function. Although some differences between the two transfer functions are found in regions of low signal (e.g., near antiresonances), the responses near resonances are nearly identical. This suggests that within the range of forces applied to the wing, non-linear processes do not have a major effect on the wing dynamics.

2. Left-Hand and Right-Hand Wing Response

The two wings of the Baron aircraft are not identical in design. Differences in the structures exist because of instrumentation asymmetries as well as physical access to the aircraft; for example, the skin near the inboard edge of the right wing is stiffened to support passenger weight while accessing the forward cabin door. Additionally, the extent of damage on both wings is different.

Modal tests on both left-hand and right-hand wings were performed to evaluate the effect of these differences on the low frequency wing dynamics. Each wing was freely-supported using air-filled tubes distributed along the wing. Neither wing had an engine mount attached.

Results for a transfer function to the forward and rear spars of both wings are shown respectively on Figs. A-4a and A-4b. The shapes of the curves obtained for each wing are similar and several of the resonance peaks occur at nearly the same frequency. Differences are found in the number of resonance peaks as well as relative amplitude. In general however these results indicate that the structural differences between the wings do not radically alter their low frequency dynamic response.

3. Support Configuration

During most of the testing of the Baron aircraft the wings were supported on air-filled tubes distributed along the wing. The precise location of these tubes was neither monitored nor adhered to during changes in configuration. While the position of the soft supports would not likely

be a major influence on the response of the larger structural members of the wing (e.g., spars and ribs), it was recognized that the static tension in the wing skin would be influenced by the configuration of the supports.

The sensitivity of the wing dynamics to the configuration of the air-filled tubes was evaluated by performing a modal analysis on the right-hand wing with tubes positioned only along the root and tip wing edges. In this configuration in which the static weight of the wing is only supported at the edges, the skin along the lower wing surface is placed in tension while that on the upper surface is placed in compression.

Results of this configuration are compared on Figs. A-4a and A-4b with those of the more common test configuration in which the supporting tubes are distributed along the entire wing surface. The two fundamental frequencies at 45 Hz (bending) and at 54 Hz (torsion) are minimally effected by the support configuration. Differences are found in the location of the higher order resonance peaks although the overall character of the two transfer functions remains similar.

Based on this comparison we conclude that the static support configuration of the wing has some influence on the higher order resonance frequencies of the wing.

TABLE A-I
 RESONANCE FREQUENCIES AND MODAL LOSS FACTORS OF
 THE FREELY-SUPPORTED WING

<u>Mode No.</u>	<u>Without Engine Mount</u>		<u>With Engine Mount</u>	
	<u>Frequency</u>	<u>Damping</u>	<u>Frequency</u>	<u>Damping</u>
1	45.2 Hz	0.016	45.5 Hz	0.006
2	53.6 Hz	0.042	53.0 Hz	0.017
3	68.0 Hz	0.017	66.7 Hz	0.015
4	74.7 Hz	0.032	71.8 Hz	0.045
5	87.2 Hz	0.037	84.8 Hz	0.028
6	103.8 Hz	0.019	95.2 Hz	0.051
7	108.8 Hz	0.029	103.0 Hz	0.045
8	120.6 Hz	0.045	104.0 Hz	0.028
9	132.0 Hz	0.027	116.8 Hz	0.037
10	137.6 Hz	0.076	118.6 Hz	0.022
11	—	—	131.5 Hz	0.024
12	—	—	142.9 Hz	0.046

TABLE A-II
 RESONANCE FREQUENCIES AND MODAL LOSS FACTORS OF
 THE WING WITH ENGINE MOUNT WHEN ATTACHED TO THE FUSELAGE

<u>Mode No.</u>	<u>Frequency</u>	<u>Damping</u>
1	3.8 Hz	0.23
2	6.4 Hz	0.14
3	11.6 Hz	0.13
4	16.9 Hz	0.052
5	21.6 Hz	0.017
6	25.6 Hz	0.039
7	31.7 Hz	0.037
8	36.7 Hz	0.045
9	37.7 Hz	0.031
10	40.3 Hz	0.007
11	49.0 Hz	0.056
12	55.6 Hz	0.037
13	57.2 Hz	0.041

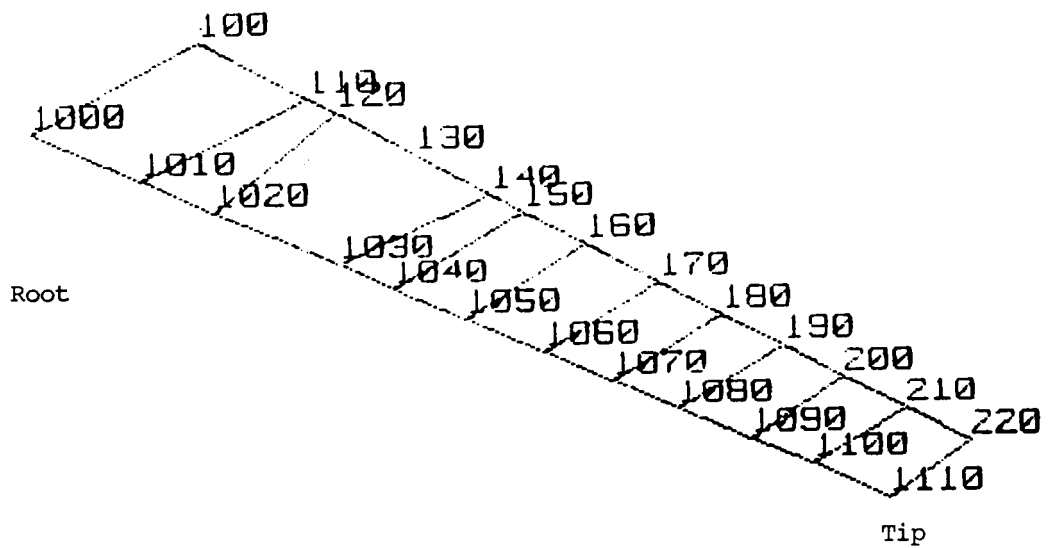


Fig. A-1 Schematic diagram showing wing locations used in modal testing.

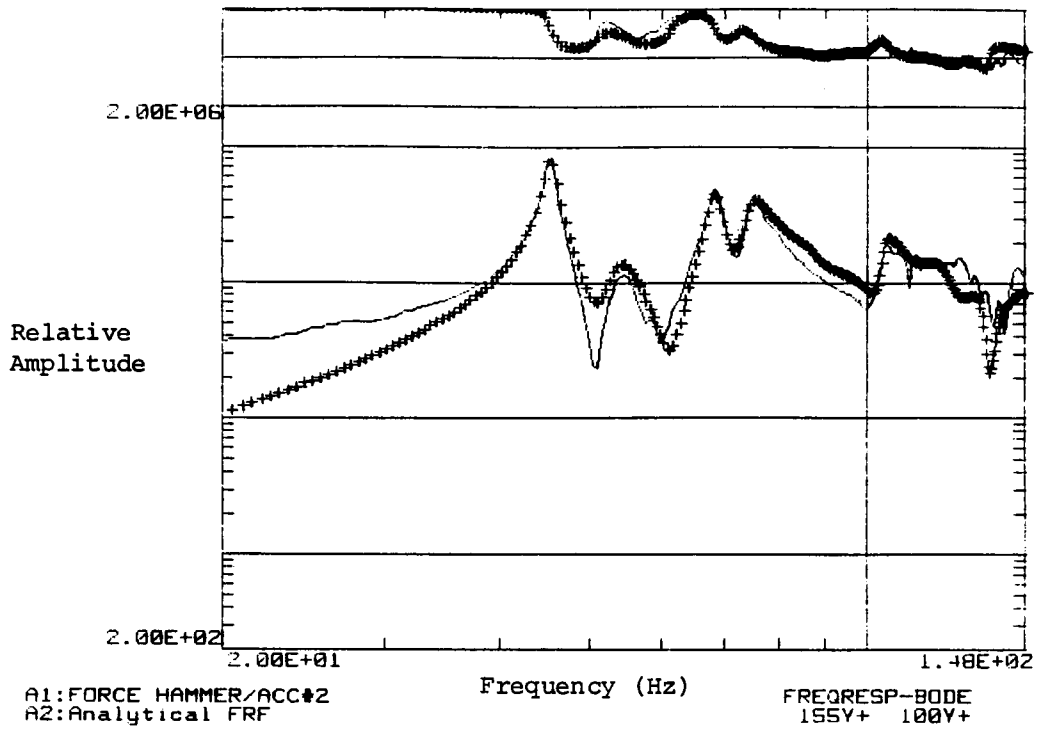
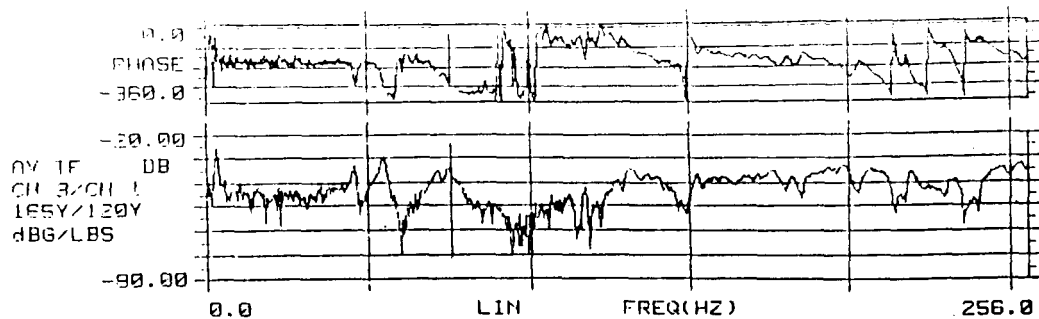
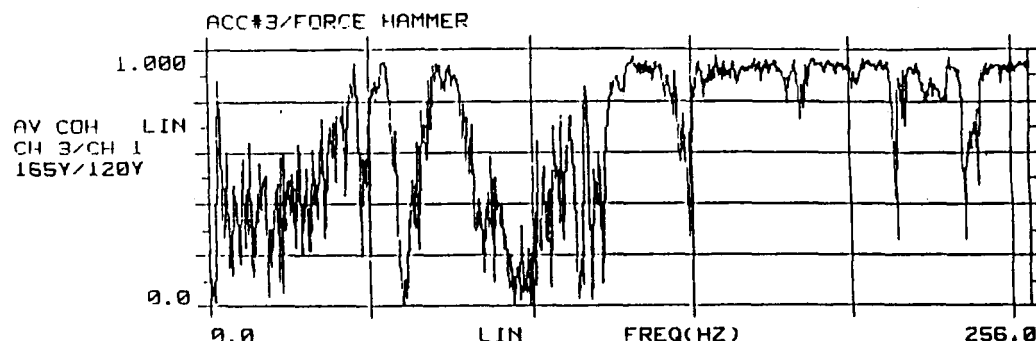


Fig. A-2 Comparison of measured (—) and curve fit (++++) transfer functions between excitation at location 100 and response at location 155 for the freely supported wing with attached engine mount.

Transfer Function



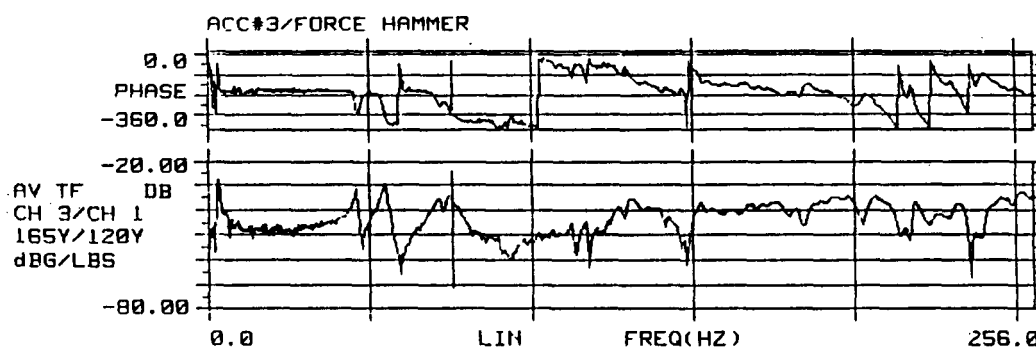
Coherence



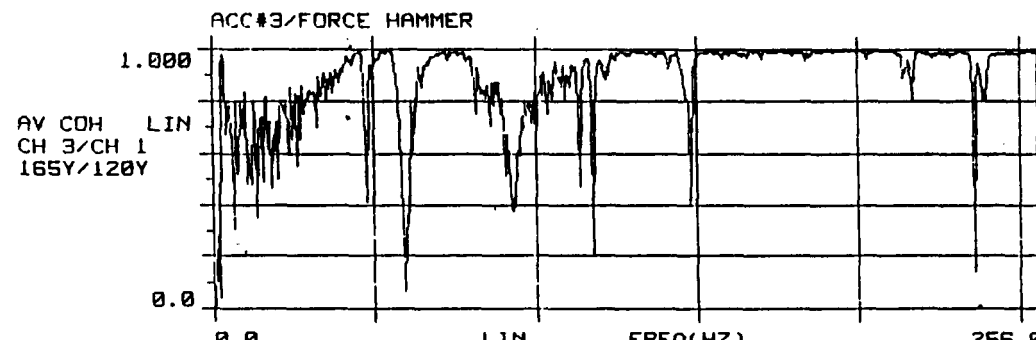
FREQ(HZ): 75.50 AMPL: -36.90 PHASE: -284.6

(a)

Transfer Function



Coherence



FREQ(HZ): 75.50 AMPL: -36.56 PHASE: -297.6

(b)

Fig. A-3 Comparison of transfer functions and coherence for the freely-supported right wing obtained using a normal hammer impact (a) and an impact having 10 times greater force (b).

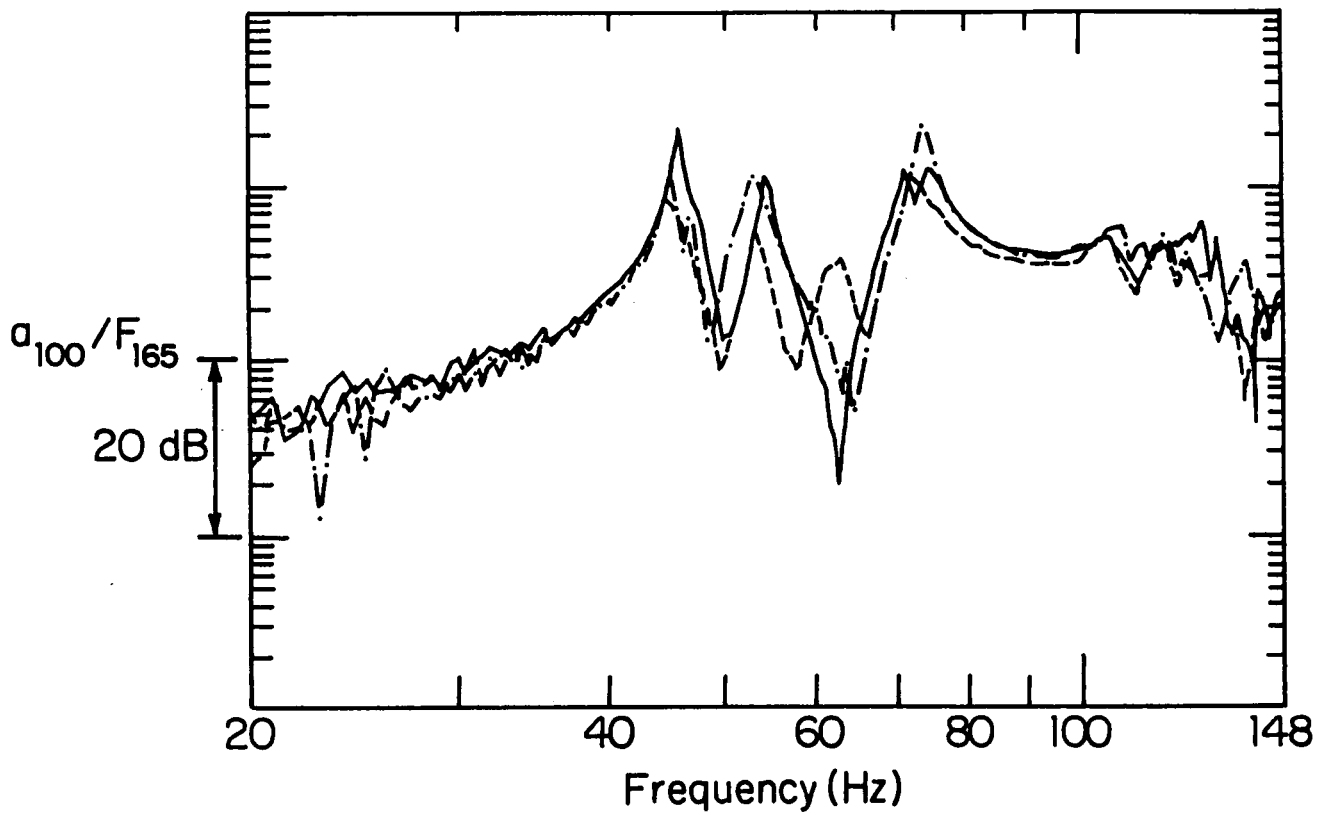


Fig. A-4a Transfer accelerance between forward spar excitation and forward spar response. (—, right wing with distributed support; —.—, left wing with distributed support; - - -, right wing with edge support).

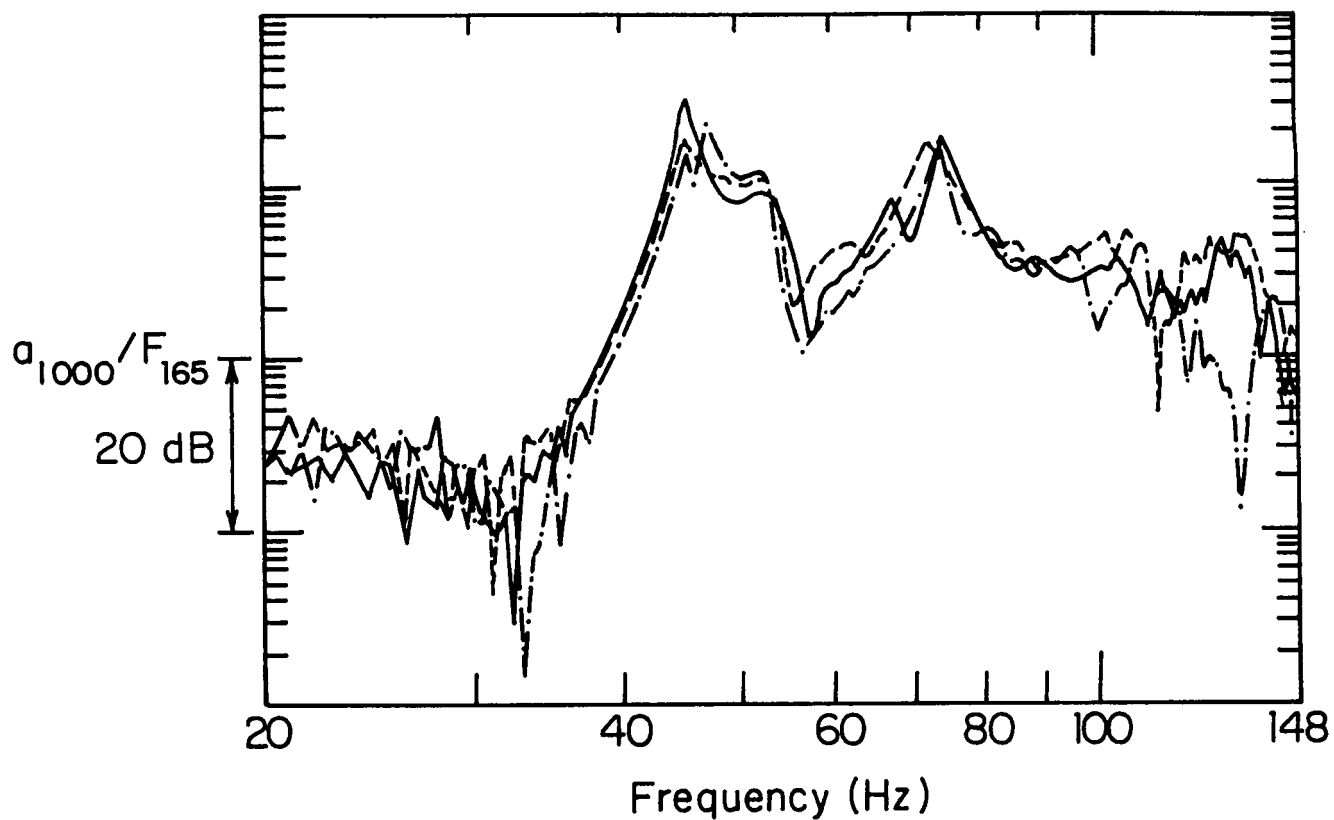
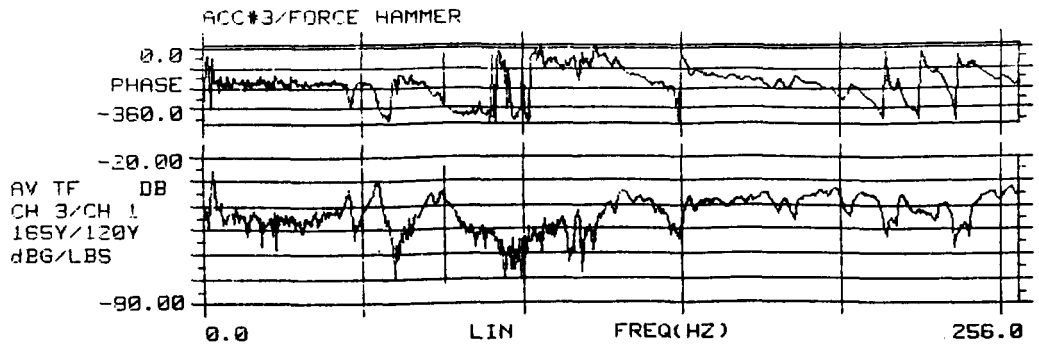
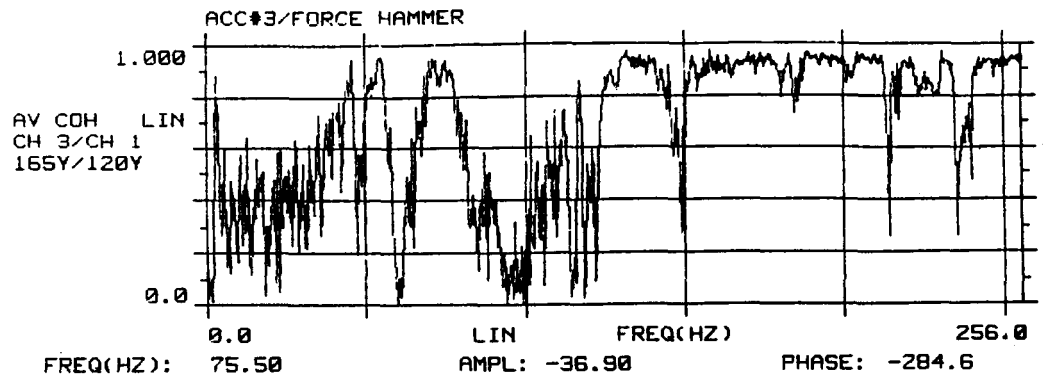


Fig. A-4b Transfer acceleration between forward spar excitation and aft spar response. (—, right wing with distributed support; — — —, left wing with distributed support; - - -, right wing with edge support).

Transfer Function

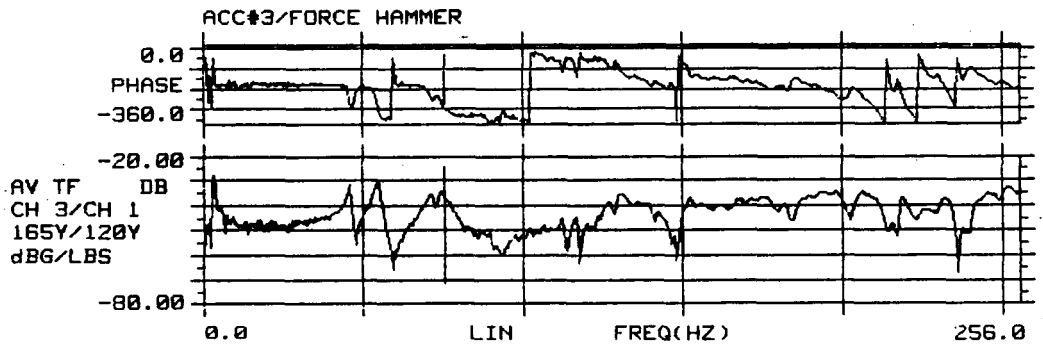


Coherence

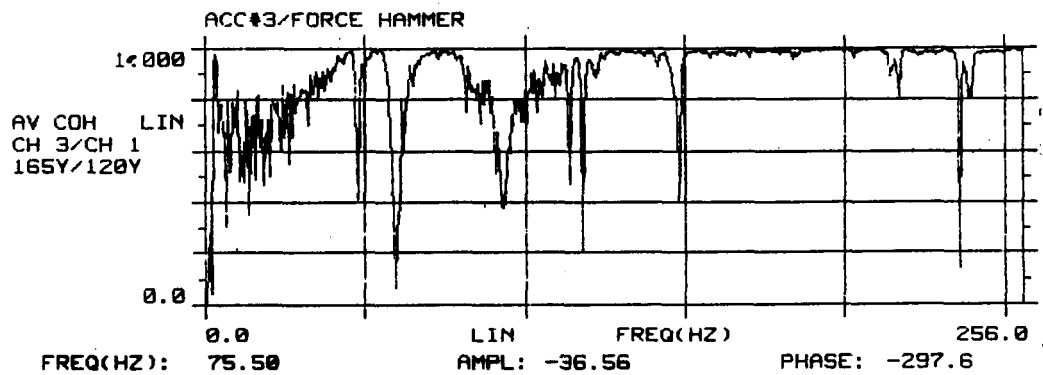


(a)

Transfer Function



Coherence

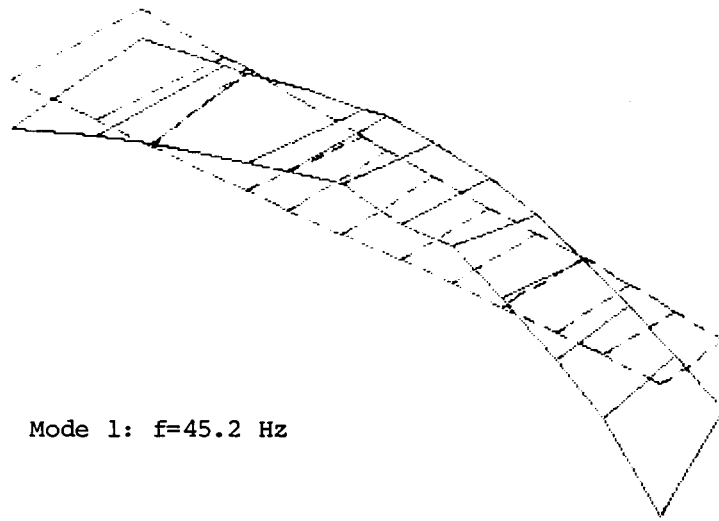


(b)

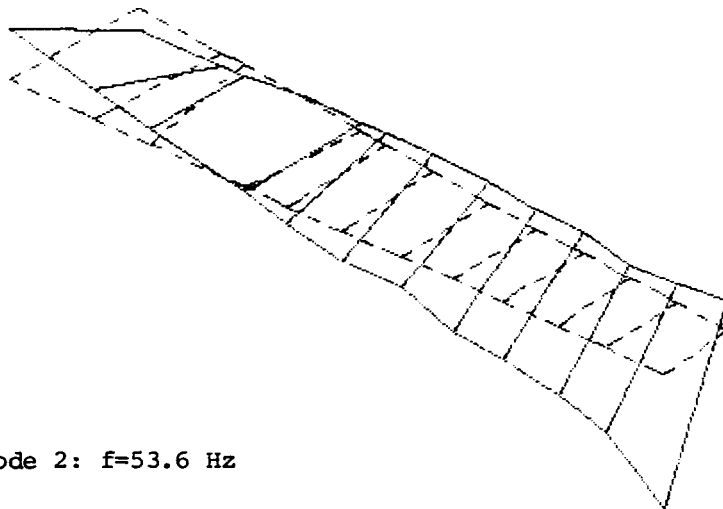
Fig. A-5 Comparison of transfer functions and coherence for the freely supported right wing obtained using a normal hammer impact (a) and an impact having 10 times greater force (b).

APPENDIX B

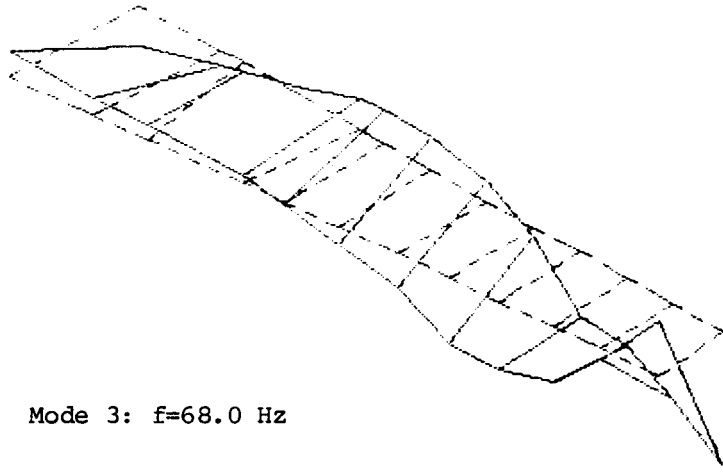
MODE SHAPES FOR WING WITHOUT ENGINE MOUNT WHEN
FREELY-SUPPORTED



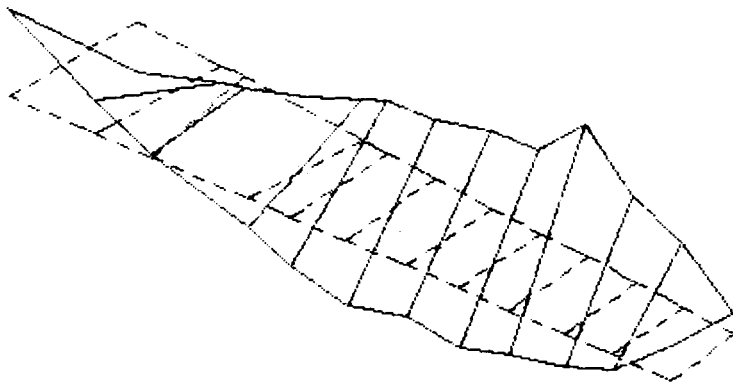
Mode 1: $f=45.2$ Hz



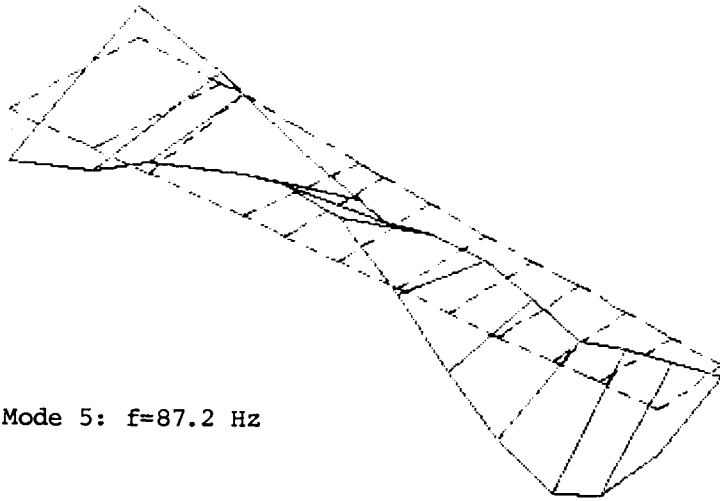
Mode 2: $f=53.6$ Hz



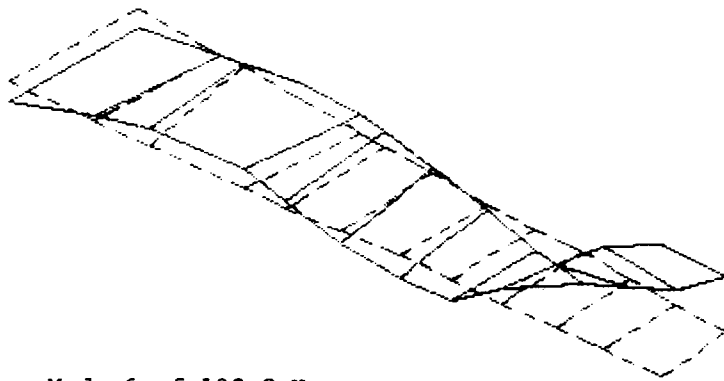
Mode 3: $f=68.0$ Hz



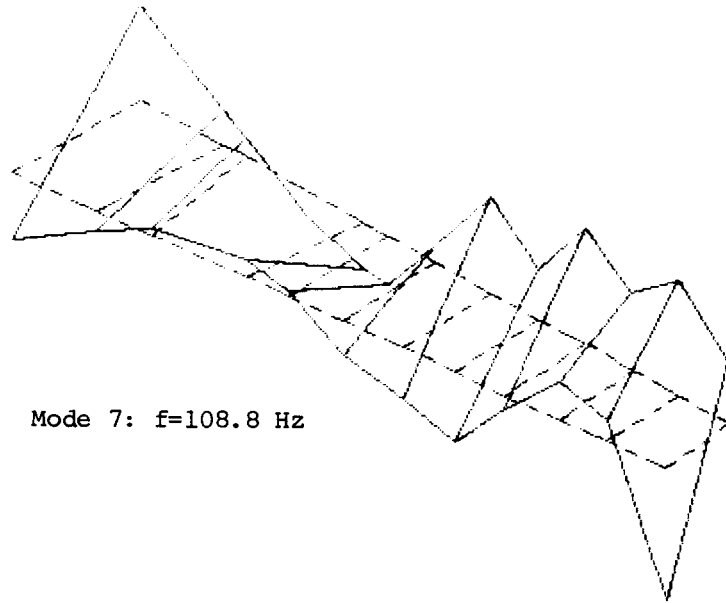
Mode 4: $f=74.7$ Hz



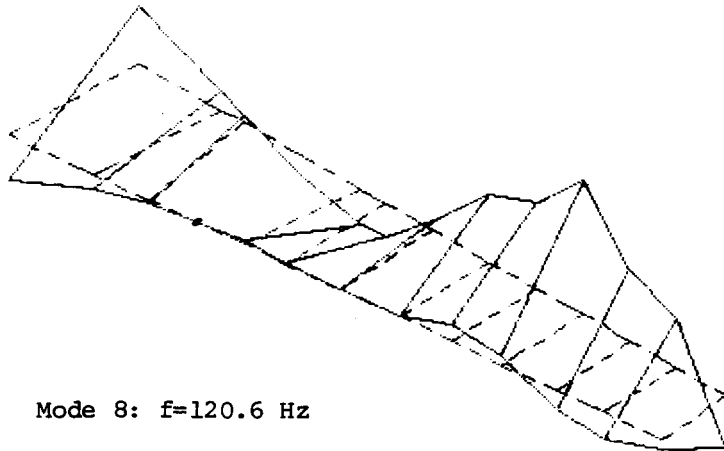
Mode 5: $f=87.2$ Hz



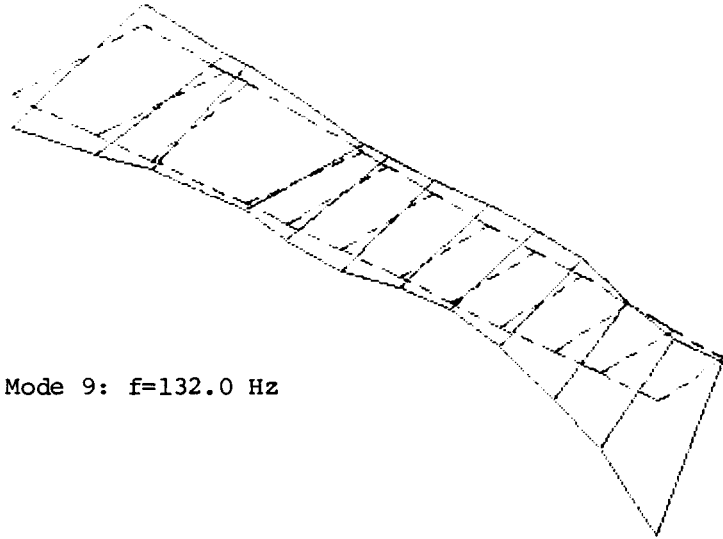
Mode 6: $f=103.8$ Hz



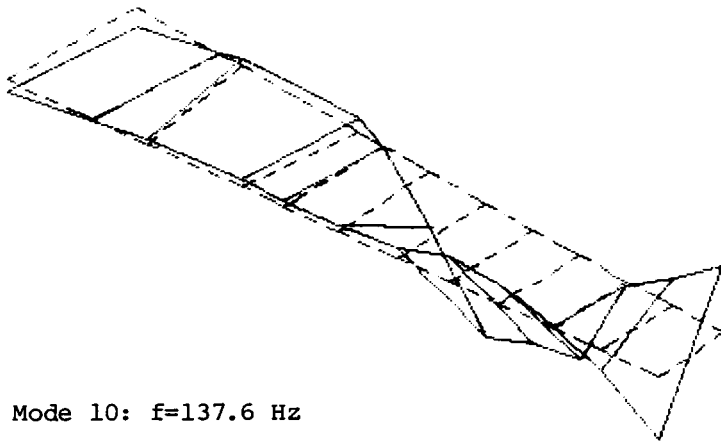
Mode 7: $f=108.8$ Hz



Mode 8: $f=120.6$ Hz



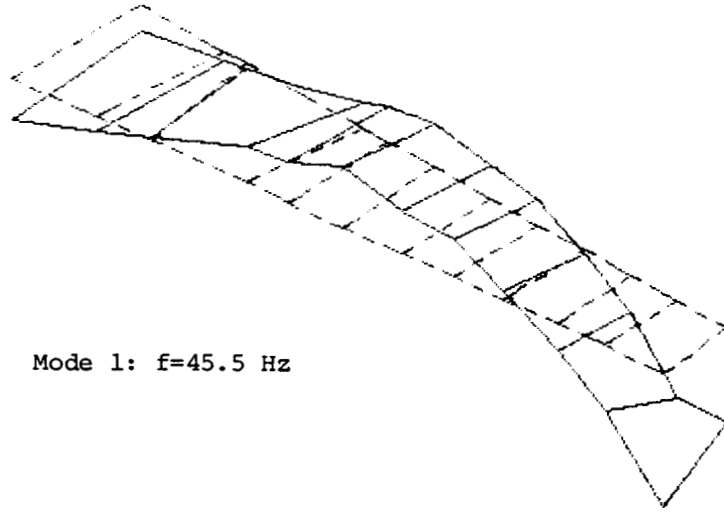
Mode 9: $f=132.0$ Hz



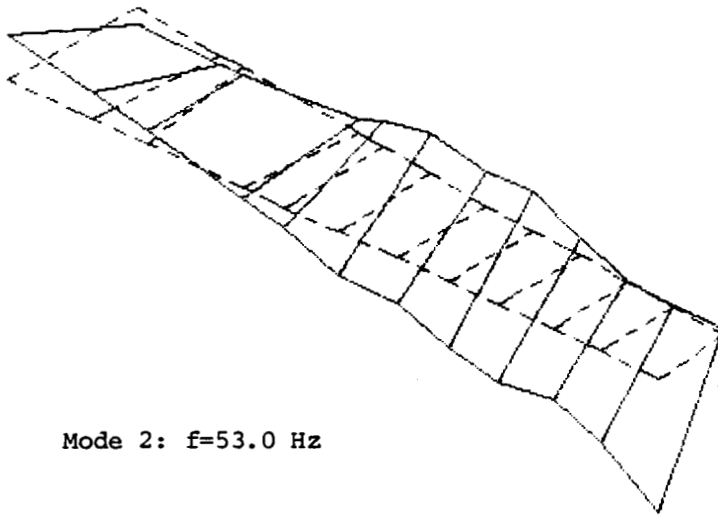
Mode 10: $f=137.6$ Hz

APPENDIX C

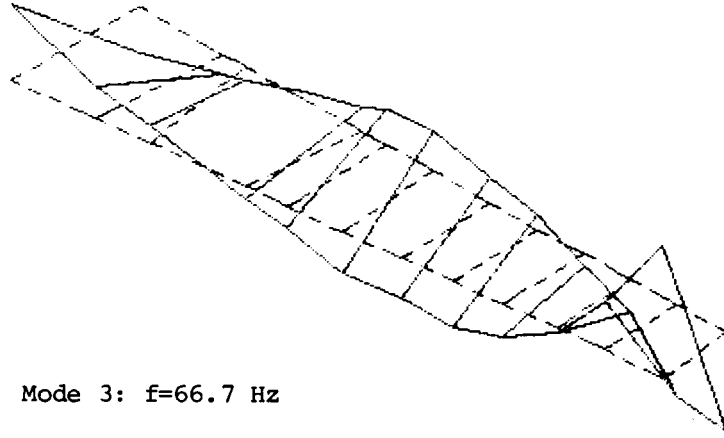
MODE SHAPES FOR WING WITH ENGINE MOUNT WHEN FREELY-SUPPORTED



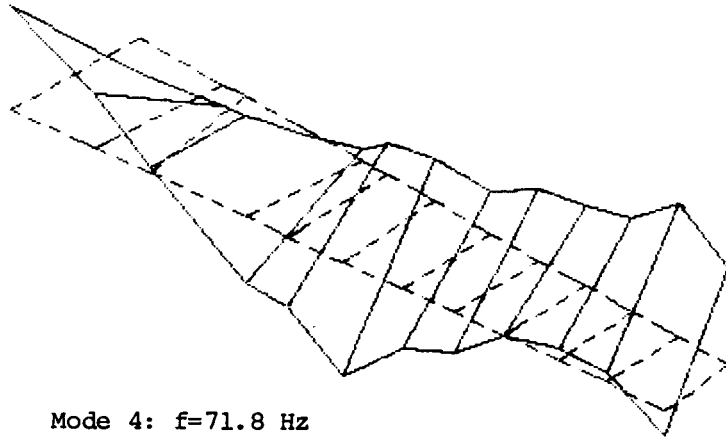
Mode 1: $f=45.5$ Hz



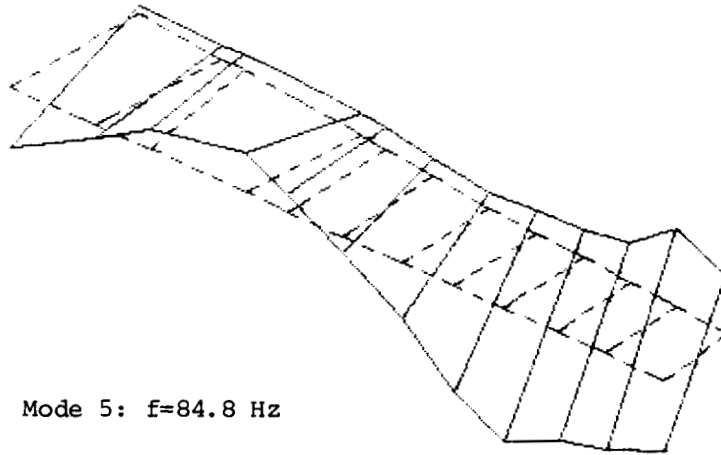
Mode 2: $f=53.0$ Hz



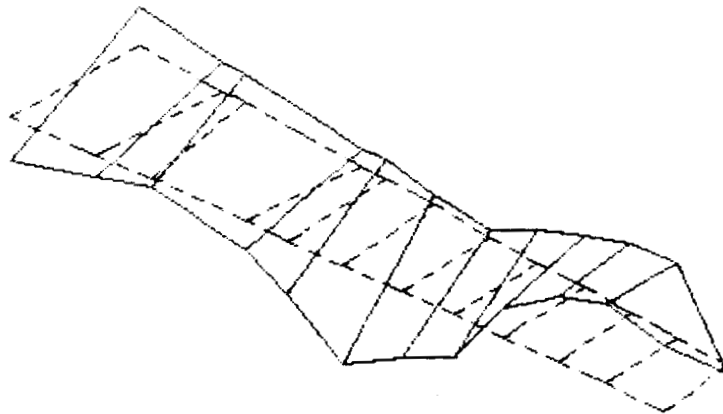
Mode 3: $f=66.7$ Hz



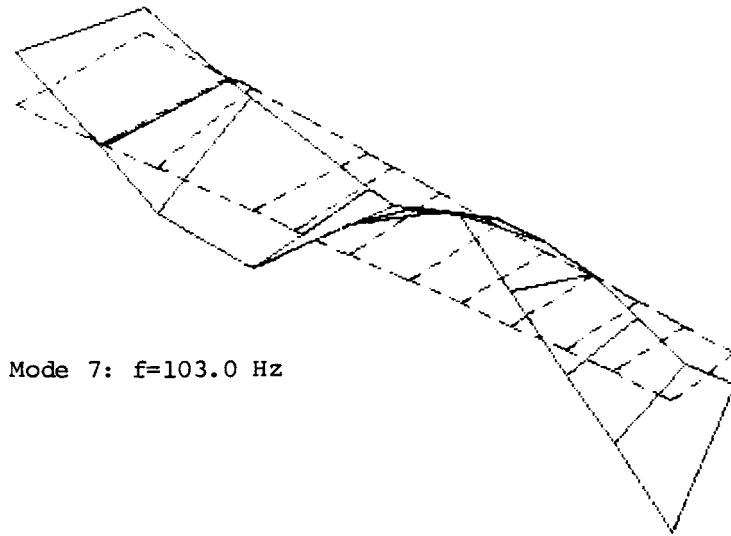
Mode 4: $f=71.8$ Hz



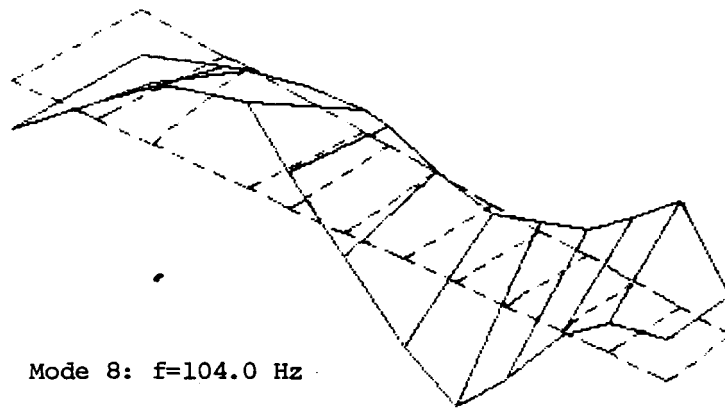
Mode 5: $f=84.8$ Hz



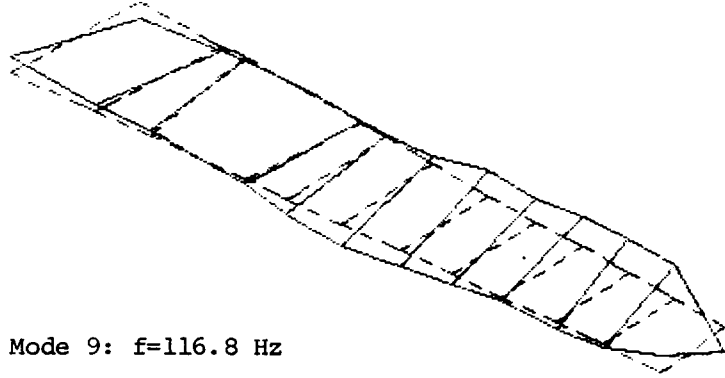
Mode 6: $f=95.2$ Hz



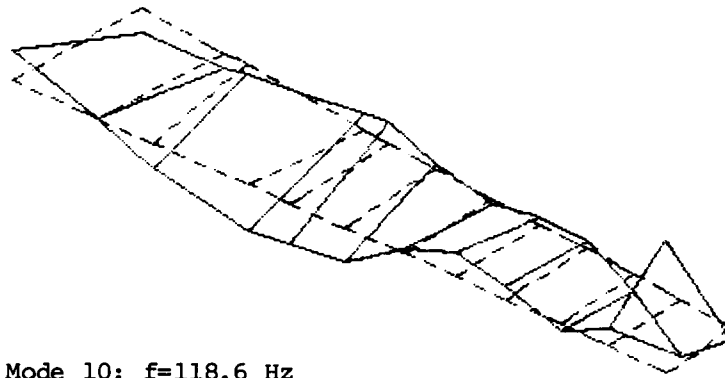
Mode 7: $f=103.0$ Hz



Mode 8: $f=104.0$ Hz



Mode 9: $f=116.8$ Hz

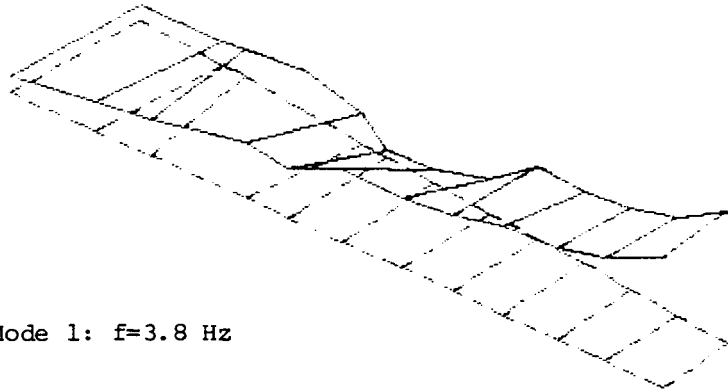


Mode 10: $f=118.6$ Hz

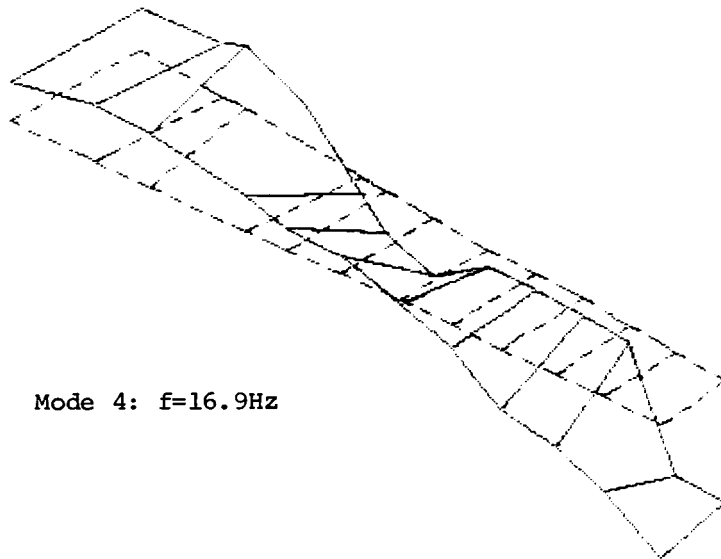
APPENDIX D

MODE SHAPES* FOR WING WITH ENGINE MOUNT WHEN
BOLTED TO FUSELAGE

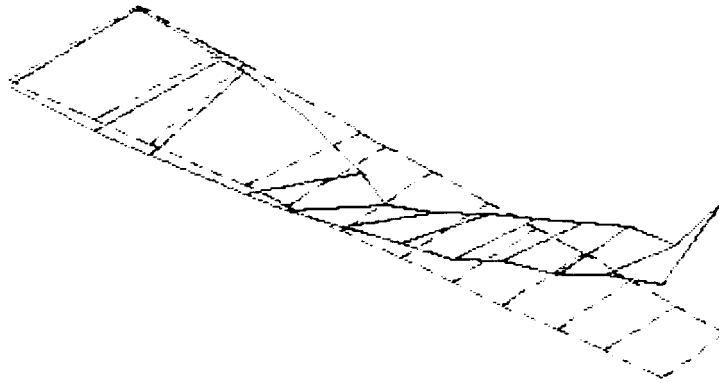
* Shapes for mode 2 and 3 not included.



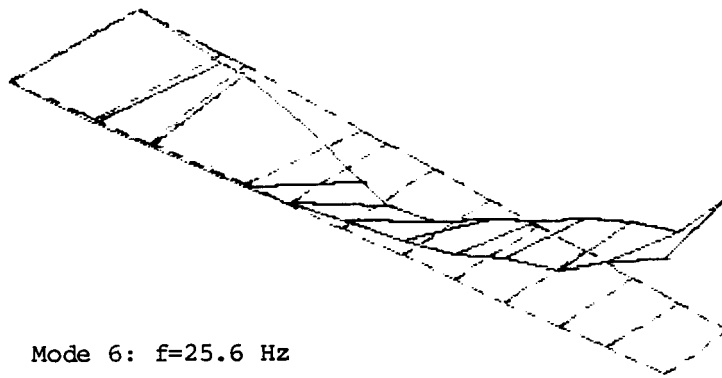
Mode 1: $f=3.8$ Hz



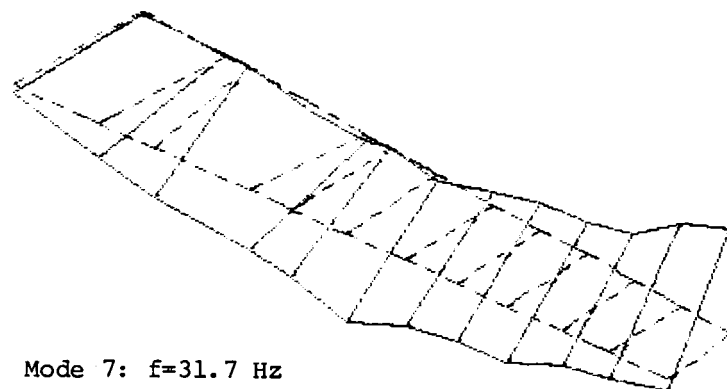
Mode 4: $f=16.9$ Hz



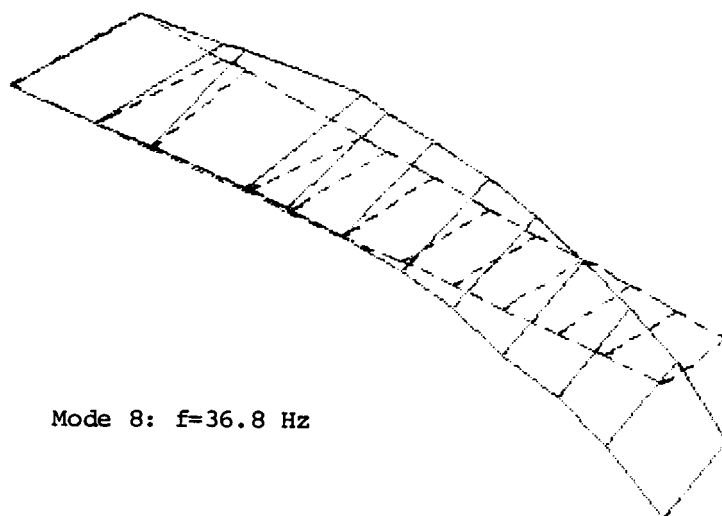
Mode 5: $f=21.5$ Hz



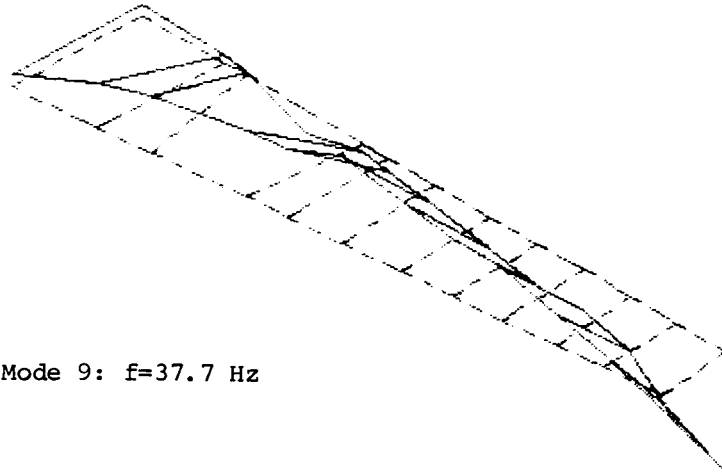
Mode 6: $f=25.6$ Hz



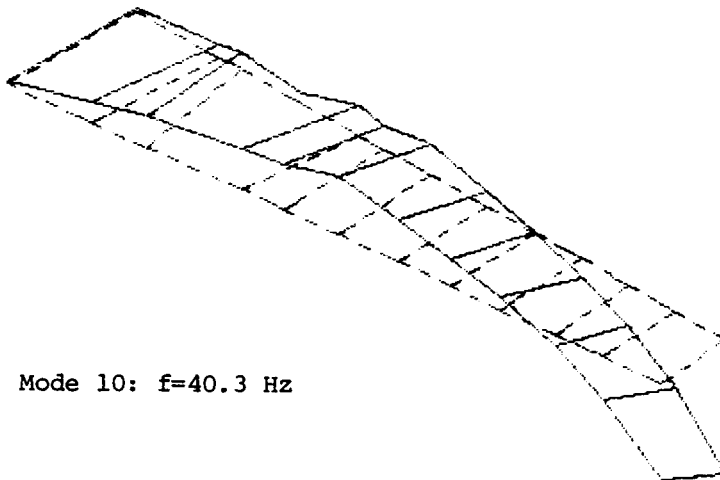
Mode 7: $f=31.7$ Hz



Mode 8: $f=36.8$ Hz



Mode 9: $f=37.7$ Hz



Mode 10: $f=40.3$ Hz



Report Documentation Page

1. Report No. NASA CR-4137		2. Government Accession No.		3. Recipient's Catalog No.	
4. Title and Subtitle Structureborne Noise Measurements on a Small Twin-Engine Aircraft				5. Report Date June 1988	
				6. Performing Organization Code	
7. Author(s) J. E. Cole III and K. F. Martini				8. Performing Organization Report No. U-1541-349 Part II	
				10. Work Unit No. 535-03-11-03	
9. Performing Organization Name and Address Cambridge Acoustical Associates, Inc. 80 Sherman Street Cambridge, MA 02140				11. Contract or Grant No. NAS1-18020	
				13. Type of Report and Period Covered Contractor Report	
12. Sponsoring Agency Name and Address National Aeronautics and Space Administration Langley Research Center Hampton, VA 23665-5225				14. Sponsoring Agency Code	
				15. Supplementary Notes Langley Technical Monitor: William H. Mayes	
16. Abstract <p>Structureborne noise measurements performed on a twin engine aircraft (Beechcraft Baron) are reported. There are two overall objectives of the test program. The first is to obtain data to support the development of analytical models of the wing and fuselage, while the second is to evaluate effects of structural parameters on cabin noise. Measurements performed include structural and acoustic responses to impact excitation, structural and acoustic loss factors, and modal parameters of the wing. Path alterations include added mass to simulate fuel, variations in torque of bolts joining wing and fuselage, and increased acoustic absorption. Conclusions drawn regarding these measurements are presented.</p>					
17. Key Words (Suggested by Author(s)) Structureborne Noise Propeller Noise Aircraft Vibrations and Noise Cabin Interior Noise			18. Distribution Statement Unclassified - Unlimited Subject Category 71		
19. Security Classif. (of this report) Unclassified		20. Security Classif. (of this page) Unclassified		21. No. of pages 80	22. Price A05